

POLITECNICO DI TORINO

**Corso di Laurea Magistrale
in Ingegneria Aerospaziale**

Tesi di Laurea Magistrale

**A Multidisciplinary Framework for Aircraft
Landing Gear Brake Actuation Design**



Relatori

Prof. Paolo Maggiore

Dott. Ing. Laura Mainini

Candidato

Simone Tumiatì

Tumiatì Simone

Dicembre 2018

UTC Proprietary

This material contains proprietary information of United Technologies Corporation. Any copying, distribution, or dissemination of the contents of this material is strictly prohibited and may be unlawful without the express written permission of UTC. If you have obtained this material in error, please notify UTRC Counsel at (860) 610-7948 immediately.

Created at UTRC-Ireland

EU export classification: ECCN NSR. The content of this document is not controlled by EU dual use and/or military export control laws and regulations, but subject to general EU restrictive measures in place (article 215 TFEU).

Contents

LIST OF FIGURES	5
LIST OF TABLES	7
GLOSSARY	8
ABSTRACT	9
1. INTRODUCTION	10
1.1 Overview	10
1.2 Problem Statement	13
2. BACKGROUND AND STATE OF ART	17
3. BRAKE ACTUATION SYSTEM DESIGN	18
3.1 Generic Brake Configuration	18
3.2 Architecture Definition.....	22
3.2.1 <i>Architecture Exploration</i>	23
3.2.2 <i>Architecture Evaluation</i>	25
3.2.3 <i>Architecture Localization</i>	27
3.3 System Sizing.....	28
3.3.1 <i>Classical Method</i>	31
3.3.2 <i>Similarity Law Method</i>	32
3.4 System Modelling and Simulation	37
3.4.1 <i>Modelling Tools</i>	37
3.4.2 <i>Hierarchical Modelling</i>	40
3.4.3 <i>Library Comparison</i>	46
3.4.4 <i>Actuator Comparison</i>	60
3.4.5 <i>Formal Requirement Models</i>	66
4. DESIGN OPTIMIZATION	71
4.1 Generic Optimization Workflow	71
4.2 Multi-Objective Optimization Problem.....	73
4.3 Optimization Implementation.....	74
4.3.1 <i>Choice of Design Variables and Constraints</i>	74
4.3.2 <i>Optimization Objective and Case Study</i>	75

5. CONCLUSIONS AND FUTURE WORK..... 82
REFERENCES 83

LIST OF FIGURES

Figure 1.1: Life cycle cost diagram ^[2]	10
Figure 1.2: Overview of MISSION platform ^[3]	11
Figure 1.3: V-model ^[54]	14
Figure 1.4: General workflow of the Brake System design.....	15
Figure 3.1: Power brake system on a Boeing B-737 ^[20]	18
Figure 3.2: Rolling stock of multiple disc brake ^[21]	19
Figure 3.3: A flapper-nozzle servo-valve ^[22]	20
Figure 3.4: Scheme of an EMA servo-actuator ^[23]	21
Figure 3.5: Scheme of an EHA ^[23]	22
Figure 3.6: Illustration of the AEE method ^[25]	24
Figure 3.7: Schematic of the power platform data flow ^{[24][26]}	26
Figure 3.8: Comparison of electric actuator to the baseline ^[24]	27
Figure 3.9: Comparison of hybrid architectures with distributed hydraulic and electric power ^[24]	28
Figure 3.10: System sizing logical flow	29
Figure 3.11: Logical flow of the EHA sizing process	31
Figure 3.12: Translation between physical model and simulation one	38
Figure 3.13: Example of signal-oriented model ^[35]	38
Figure 3.14: FMI Code Export for Model Exchange ^[35]	39
Figure 3.15: Spring-damper oscillator exported as FMU	40
Figure 3.16: Graphical representation of partial models and interfaces	41
Figure 3.17: Implementation of the two hydraulic valve models	42
Figure 3.18: External and internal view of the valve partial model	43
Figure 3.19: Real valve representation (up) ^[36] and dynamics model (down).....	44
Figure 3.20: Piston stroke of the two valves	45
Figure 3.21: Pressure drop of the two valves	46
Figure 3.22: Custom electric motor model.....	48
Figure 3.23: Servo-motor application model.....	48
Figure 3.24: Servo-motor internal view ^[35]	49
Figure 3.25: Motor torque of the two different motor models	50
Figure 3.26: Motor shaft speed of the two motor models.....	50
Figure 3.27: Draft of OpenHydraulic (left) and SimulationX (right) libraries	52
Figure 3.28: EHA model realized with OpenHydraulics.....	53
Figure 3.29: Stroke function ^[35]	55
Figure 3.30: Internal view of the 4/3 proportional control valve ^[35]	56
Figure 3.31: Scheme of a single-acting cylinder	56
Figure 3.32: Volume flow of the two directional-control valves	58
Figure 3.33: Pressure drop of the two directional-control valves.....	59
Figure 3.34: Example of regression tests on the cylinder (left) and on the hydraulic valve (right)	60

Figure 3.35: EHA model	61
Figure 3.36: SHA model.....	62
Figure 3.37: Slip characteristic curve ^[38]	63
Figure 3.38: Internal structure of the disk brake	64
Figure 3.39: Piston stroke of the two actuator models	65
Figure 3.40: Wheel rotational speed of the brake of the two actuator models	65
Figure 3.41: MI-5 landing gear requirement model	67
Figure 3.42: MI-6 landing gear requirement model	67
Figure 3.43: EHA model with the MI-6 landing gear requirement model	68
Figure 3.44: Braking force on the wheel	69
Figure 3.45: Requirement satisfaction in percentage	70
Figure 4.1: Optimization workflow	72
Figure 4.2: Multi-objective optimization logical flowchart ^[43]	74
Figure 4.3: General template of OptiSLang	76
Figure 4.4: Complete optimization implementation template	77
Figure 4.5: CoI as a function of the objective function (Study Case 1)	78
Figure 4.6: CoI as a function of the constraint (Study Case 1).....	79
Figure 4.7: CoI as a function of the objective function (Study Case 2)	80
Figure 4.8: CoI as a function of the constraint (Study Case 2).....	81

LIST OF TABLES

Table 3.1: Similarity laws of motor parameters^[33] 34

Table 3.2: Key design drivers values (1) 35

Table 3.3: Key design drivers (2) 36

Table 3.4: Typical parameter settings for dx_h ^[35] 57

Table 3.5: Values of the four parameters of the slip curve^[38] 63

Table 4.1: Design variables and constraint of the optimization problem 75

Table 4.2: Optimization results of the Study Case 1 79

Table 4.3: Optimization results of the Study Case 2 81

GLOSSARY

A-2015	ACTUATION2015
A/C	Aircraft
AEE	Architecture Exploration and Enumeration/Evaluation
CoD	Coefficient of Determination
CoI	Coefficient of Importance
DoE	Design of Experiments
EHA	Electro-Hydrostatic Actuator
EMA	Electro-Mechanical Actuator
FAA	Federal Aviation Administration
FAR	Federal Aviation Regulation
FCC	Flight Control Computer
FMI	Functional Mockup Interface
FMU	Functional Mock-up Unit
LG	Landing Gear
MISSION	Modelling and Simulation tools for Systems IntegratiON on Aircraft
MOO	Multi-Objective Optimization
PFCS	Primary Flight Control System
RTO	Reject Take-Off
SHA	Servo-Hydraulic Actuator
UTRC-I	United Technologies Research Centre-Ireland

ABSTRACT

Modern and complex aerospace systems are being developed and optimized to enable the transition towards *more-electric* and/or *all-electric* aircraft. The integration of these systems in new generation aircraft and the multi-physics interactions between them are causing a greater complexity in both the design and verification processes. To face this complexity, several tools that can support integrated modelling, simulation, optimization and testing across all the stages of the system design are being developed. In this context, the European Commission launched the *Clean Sky 2* Joint Technology Initiative. This program is a public-private partnership which provides funding for research and development of the processes, tools and technologies that will enable the aviation industry to increase the demand for aircraft with reduced fuel consumption, noise and emission of pollutants. Under this initiative, the *Modelling and Simulation tools for Systems IntegratiON on Aircraft* (MISSION) project aims to develop and demonstrate an integrated modeling, simulation, design and optimization framework incorporating model-based systems engineering principles.

This thesis discusses the activities under the MISSION project and proposes a design platform including models library for landing gear brake system design, especially for the integration in a multidisciplinary design framework. In particular, physics-based models of different types of actuator for the landing gear brake system are developed, including servo-hydraulic and electro-hydrostatic actuators. These models will support sizing, evaluation and optimization tasks within the landing gear system platform, in the multidisciplinary framework.

In the document, the main steps of the aircraft brake system design process are illustrated. The first step is focused on the architecture definition, which helps to explore, evaluate and select promising architectures for the candidate brake actuation systems. The second step illustrates the sizing and physics-based modelling activities of different such actuator configurations. In particular, electro-hydrostatic actuator brakes are addressed in the study. The dynamic models are built using the standard multi-domain modelling language *Modelica*, with open and commercial tools. These physics-based model libraries are developed in a hierarchical and modular way. The sizing models are developed to estimate preliminary geometric and performance characteristics based on first order approximations and implemented in MATLAB environment. In addition, formal requirement models were developed using open Modelica libraries. The last step presents a design optimization analysis, in order to evaluate the best performances in term of mass reduction of the brake actuator using sizing and simulation models. The methodology including trade-off analysis and design optimisation is presented together with the associated results. All these activities are part of one of the work-package (System Design Activities) led by *United Technologies Research Centre – Ireland*.

1. INTRODUCTION

1.1 Overview

In view of the growing number of passengers traveling by aircraft ^[1], the aviation industries are focusing their attention on development of new generation commercial aircraft, in order to increase their performances and to meet strict requirements regarding fuel consumption, emissions and noise constraints. To pursue these goals, the modern aerospace systems integrated in the aircraft have reached a high level of complexity, both in design and development processes. They are composed of several strongly coupled subsystems and components that interact with each other and defined by a high number of variables from several domains (hydraulic, structural, thermal, and electrical). These factors obviously involve high costs in terms of design, development, integration, validation and verification processes. Therefore, the aerospace community put the attention to realize tools and efficient techniques that effectively support all stages of system design and allow to identify potential problems before physical prototypes are built and tested through expensive test campaigns. This is particularly important especially in the early stages of design, where the decisions of the system architecture will determine the future cost of the product. This result is expressed through the diagram shown below.

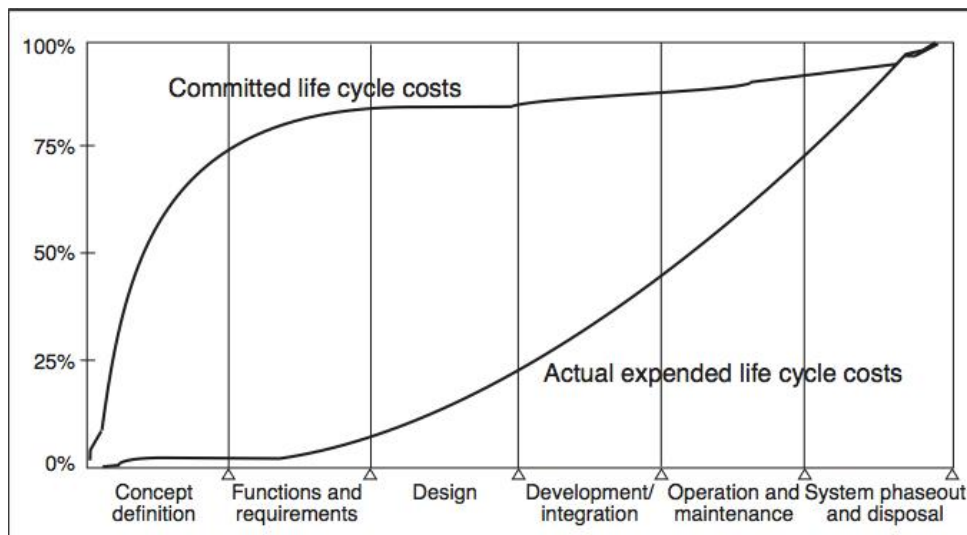


Figure 1.1: Life cycle cost diagram ^[2]

Figure 1.1 shows the *life cycle cost diagram*, which represents all costs associated with a system throughout its lifetime. The bottom curve shows the percentage of the actual, expended costs associated with a typical project. The top curve instead represents the percentage of committed costs, due to decisions and activities performed in the early phases of the system project. This diagram illustrates that over 75 % of the overall life cycle costs are locked in the design phases. The early phase activities such as understanding the problem, determining detailed functions and requirements and defining specific architectures will lock the system developers into a particular course of action, associated with specific costs. This because any changes in future life cycle phases would cause a substantial cost increase.

Consequently, the development and the application of modeling and simulation methods that support design analysis, verification and validation activities in the early design phases becomes fundamental. In this operating context, MISSION wants to realize an integrated modelling, simulation, design and optimization framework, to support holistically the entire design process, starting from conceptual design, toward capture of key requirements, system design, integration, validation and verification. **Figure 1.2** shows the complete platform envisioned in MISSION.

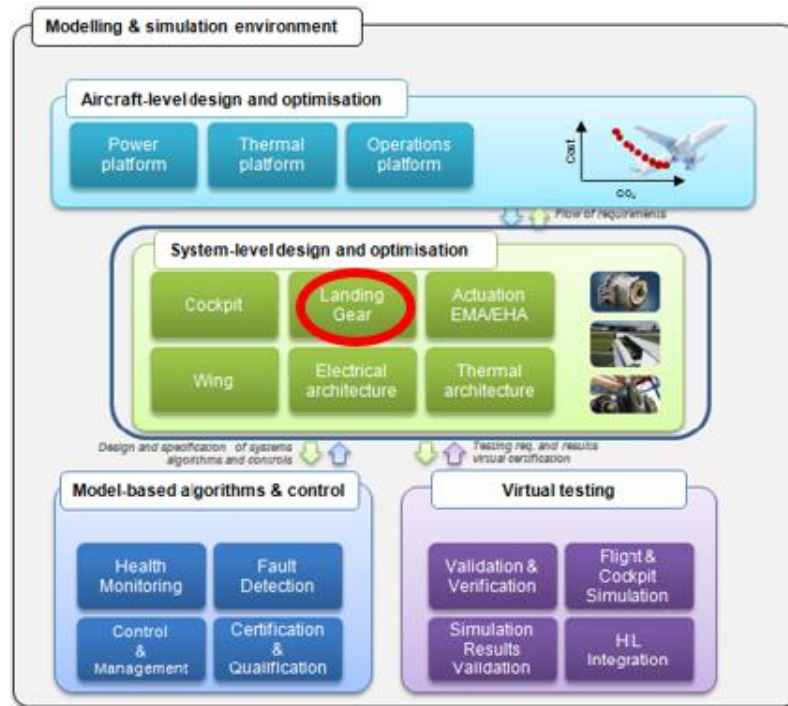


Figure 1.2: Overview of MISSION platform [\[3\]](#)

The modelling and simulation environment described in the project [\[3\]](#) focuses on different functionalities, such as model development and validation, analysis functions with optimization

capabilities, efficient data management and virtual testing. One of the most important feature of the framework proposed by the project is the use of open standard multi-domain modelling language, which is Modelica. This allows to build an open simulation environment that offers links and provides interconnections with common industry-standard tools, via the *Functional Mockup Interface* (FMI) [4]. This technique is used to define standardized interfaces in computer simulations to develop complex cyber-physical systems. A more detail description of the FMI is presented in the following sections of this document.

In the aircraft design and optimization platform, the application of multi-objective optimization analysis on a specified aircraft architecture allows to evaluate multiple aircraft design metrics such as emissions, fuel consumption and lifecycle cost, starting from high-level requirements. In particular, an A/C level modelling library is developed under MISSION to evaluate the A/C level architecture designs from a multi-domain perspective, taking into account interactions between systems. The outputs of the design will serve as requirements for the next hierarchical level, which is the system-level optimization platform. This platform includes overall multi-domain libraries of subsystems and components, as well as tools for design and optimization of different aircraft architectures, with particular attention on electrical architecture, thermal architecture, wing architecture, landing gear, actuation systems and cockpit.

MISSION delivers also an integrated framework which include a set of specifications and algorithms for controls and management, health monitoring and fault detection functions for aircraft systems and subsystems. The modelling environment related to the project includes a virtual testing platform, which enables to validate and verify the design process at multiple levels of abstraction, including partial virtual certification of aircraft components. The platform supports PC-based testing in early development phases and lab-based real-time testing of simulated real control units.

Within the multi-domain modeling and simulation platform proposed by the project, the work presented in this thesis is concentrated on the realization of a general framework of the landing gear (LG) dynamics, especially landing gear brakes, related to the system-level design platform of MISSION. In particular, the aim of this work is to provide the hierarchical libraries, presented in the system design platform, with sizing and physics-based models of different actuation systems, such as classical *servo-hydraulic actuator* (SHA) and the new *electro-hydrostatic actuator* (EHA). The application of these physics-based and parametric models includes design optimization, trade-off analysis and aircraft level integration.

1.2 Problem Statement

The high level of integration and the multi-physics interactions between components are becoming more critical as the systems are increasingly interconnected and coupled. They are characterized by different scales in space (from very big to very small components), in time (from very fast to very slow phenomena), and in function (consisting of complex hierarchies of heterogeneous functionalities). All these aspects lead to difficulties to guarantee an efficient transfer and traceability of information during all the design process.

In literature, different methods to define integrated and structured design processes are proposed, spanning from *layered design* [5][6] to *component-based* [7][8] and/or *model-based* approaches. Between these ones, the *V-model* is one of the widely used models in engineering product development related to the design process. This method [9] represents a sequential progression of plans and design stages, starting from high-level, less-detailed design stage and progressing to the low-level, more-detailed stages. The left side of the "V" represents the decomposition flow: it starts with the stakeholder needs in terms of requirements and continues with the definition of the specifications of systems and subsystems. The decomposition phase is paralleled with the right side of the model by the integration, starting from subsystem level to the final product integration. Across the cycle, it is fundamental to define the interfaces between the different phases, to assure that specifications from previous phases are captured in the following ones. In this way, changes at subsystem levels are reflected in expected changes at system and aircraft level and vice versa. Besides, each of the V-cycle phases are characterized by testing activities used to verify the compliance of the system, according to the specifications deriving from the previous phases.

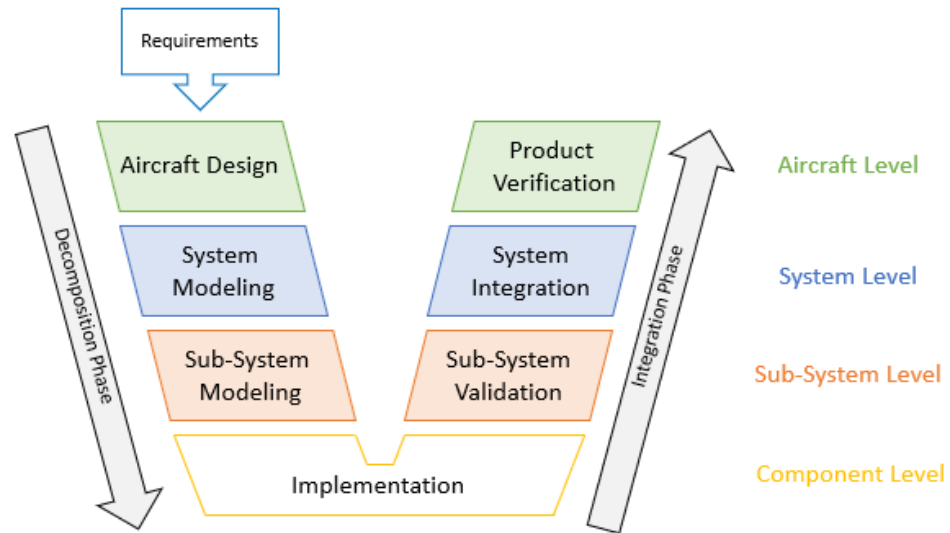


Figure 1.3: V-model [54]

MISSION adopts the V-model (**Figure 1.3**) to develop a toolchain to adequately explore, design and integrate aircraft systems to evaluate impacts from system on aircraft and vice versa, following the Clean Sky 2 objectives. The work described in this document is focused on the subsystem modelling phase, especially in the LG brake actuation system. Within this general framework, the relevant steps of the aircraft brake system design process are presented in this document, following the workflow shown in **Figure 1.4**.

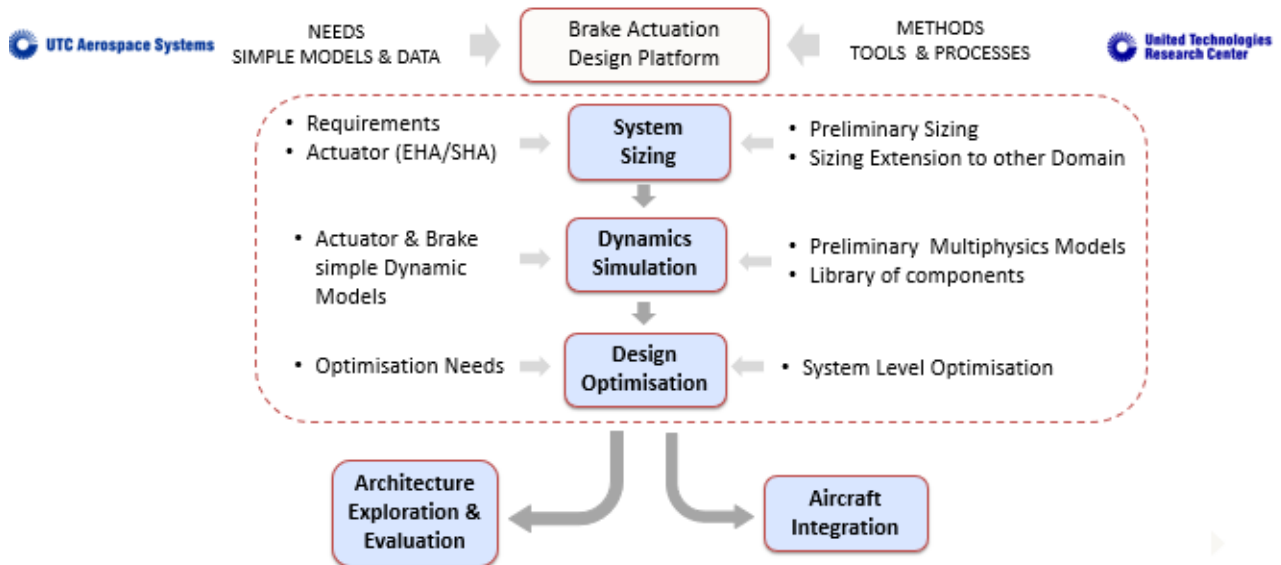


Figure 1.4: General workflow of the Brake System design

The first step is represented by the *system sizing*, which consists in develop models that allow to obtain preliminary estimates of system specifications useful for dynamics modelling and design optimization analysis. In case of actuators, these parameters can be, for example the cylinder mass, the pump displacement, the motor torque, obtained by models implemented as simple MATLAB scripts. These data will be used at this point as input to test and run all the dynamic models realized in the next phase of the design process, which is the *dynamic simulation*. Within this phase, several modelling and simulation activities are performed, such as:

- The choice of tools for modelling. In particular, all the models are built using a standard multi-domain modelling language Modelica (following the principles of MISSION) with the use of different software.
- The description of the *hierarchical modelling*, which is a modelling approach that helps in easy maintainability of different fidelity models and their use depending on intended purpose. This concept is applied to give the possibility to external users to choose between different hydraulic valves applicable in the actuator models.
- The comparison between different type of libraries to realize the models. The objective here is to verify which is the most useful and usable library for modelling, by comparing simple EHA models and electric motor ones.
- The description of the complete realization of an EHA model and a SHA one. The goal is to compare and evaluated them for successive design optimization analysis and integration at aircraft level.

- The formalisation of system requirements through the so-called *formal requirement models*, i.e. simulation models in which the system requirement is inserted and can be tested along with the simulation tools.

Once the dynamic models are built, it is possible to perform design optimization analyses in order to obtain the optimal design point with respect to both dynamic performance and non-performance characteristics, such as power consumption and mass respectively, in reference to the actuators. At the end of the design cycle proposed, the models can be integrated in the MISSION framework in order to support methodological approaches to link architecture exploration and design optimization. This process, called *Architecture Exploration and Evaluation*, is illustrated in the next sections of this document. In addition, the models can also be integrated at aircraft level to evaluate the impacts on it (in terms for example of power consumption, fuel burn, system weight) and on the other subsystems.

2. BACKGROUND AND STATE OF ART

Most of commercial aircraft in service today use the centralized hydraulic system to feed all the actuation devices, from those applied to the flight control surfaces, to those used in the landing gear dynamics. Usually, the pressurized fluid produced by an engine-driven pump acts on the cylinders to move the control surfaces of the *Flight Control System* (FCS), or to push the disks of the LG brake to reduce the rotational speed of the wheels, or also to drive the retraction/extraction system of the LG.

Recent developments in aerospace actuation systems technologies allow to substitute the hydraulic system with localized devices, such as EMA and EHA. From 20th century [\[10\]](#)[\[11\]](#), the researchers have begun to develop and use alternative methods and tools to support the design of these new type of actuation systems. Jackson D. [\[12\]](#) in his work compares a conventional hydraulic actuation and a hybrid architecture featuring both EHA's and hydraulic actuators. Fraj A. et al. [\[13\]](#) propose a simulation-based preliminary design method involving sizing of EMA's for primary flight control surface. This methodology is used to combine no-causal modeling, metamodeling and scaling laws to take advantage of simulation capabilities of recent system level simulation software. The goal is to obtain technological alternatives quantitatively from a limited set of required data, in the same way to what has been achieved through the sizing models presented in this work. Chakraborty I. et al. [\[14\]](#) show a MATLAB/Simulink methodology for the sizing, simulation, analysis, and optimization of electric actuators for the primary and second flight control surfaces of more-electric aircraft. This work focuses on the development of: the flight load estimation capability; the modelling and simulation environment where some actuator performances and thermal dynamics are analyzed; and the weight estimation method. The work describes also an actuator optimization problem for a given objective function and a set of constraints, as done in this thesis. Liscouët J. et al. [\[15\]](#) give an integrated procedure for preliminary design of EMA's in a redundant electro-mechanical nose gear steering system. The methodology proposed in the paper puts emphasis on finding the most promising candidate architectures that are compliant with the project requirements in general and the safety and reliability requirements.

Several efforts have been supported also by different European Union projects. For example, *CRESCENDO* [\[17\]](#) provides demonstrations of simulation-based product development across all the design phases. *TOICA* [\[18\]](#) develops an integrated platform for the aircraft thermal system. *MOET* [\[19\]](#) presents a framework for integration and validation of electrical technologies for more-electric aircraft.

3. BRAKE ACTUATION SYSTEM DESIGN

3.1 Generic Brake Configuration

All modern aircraft are equipped with brakes. Their main function is to guarantee safe operations of the aircraft on the ground, including (1) to slow and stop the aircraft in a reasonable amount of time, (2) to keep the aircraft positioning during engine run-up, and (3) to support steering maneuvers during taxi. The brake unit in general is mounted in each wheel of the main gear, while the nose wheel or tail wheel usually does not have a brake. In common brake system as shown in **Figure 3.1**, mechanical and/or hydraulic linkages to the rudder pedals allow the pilot to control the brakes. The basic operation of brakes involves converting the kinetic energy of motion into heat energy through the creation of friction. A significant amount of heat is developed and forces on the brake system components are demanding.

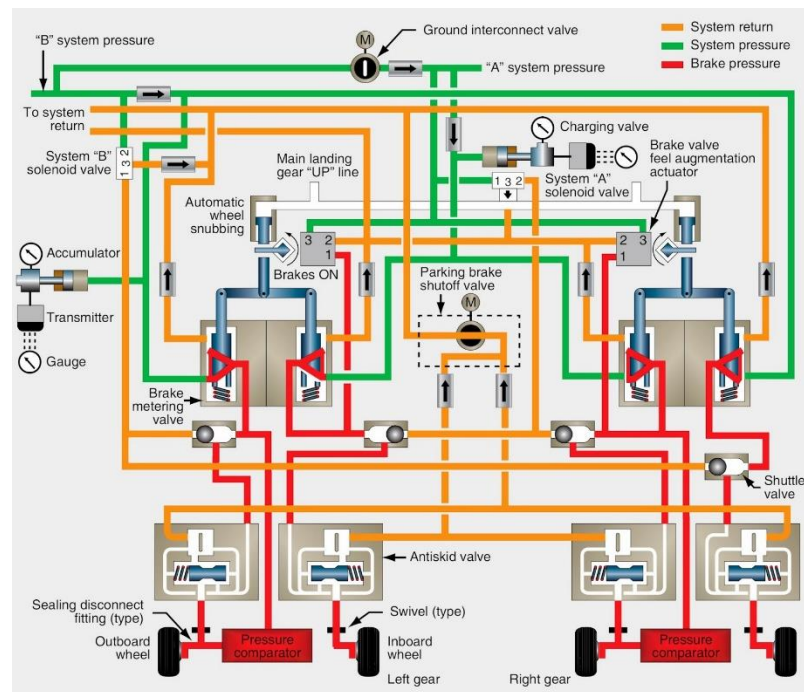


Figure 3.1: Power brake system on a Boeing B-737 [20]

Modern aircraft use disc brakes in different configurations such as single, dual or multiple discs brake.

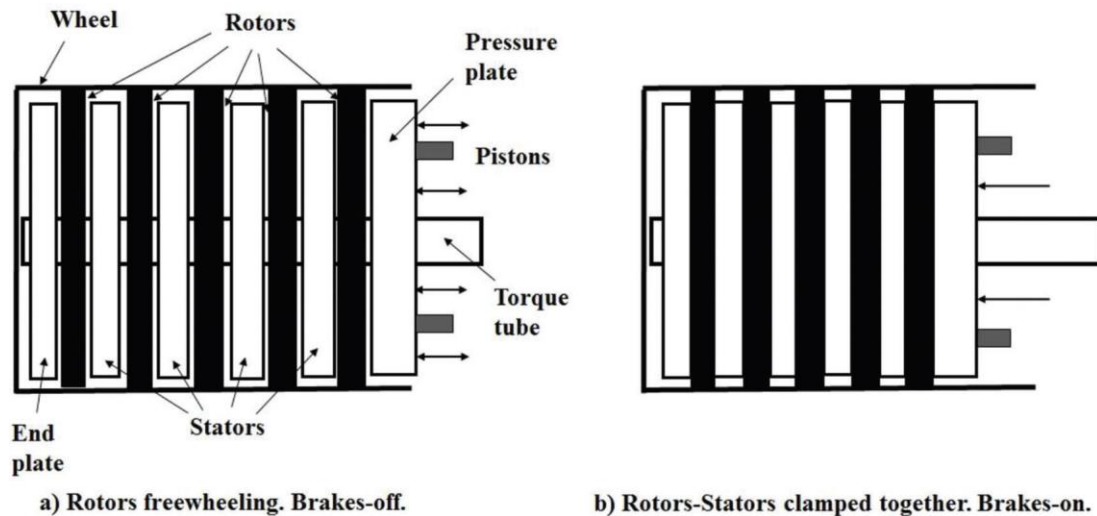


Figure 3.2: Rolling stock of multiple disc brake [\[21\]](#)

Figure 3.2 shows a simple scheme of a multiple disc, where the stators are attached to a torque tube (which is fixed and does not rotate) while the rotors spinning between the brake stators. When the breaks are activated, the actuators compress the pressure plate against the end plate. This reduces the space between the stators and rotors that, pressed against each other, produce a friction torque that decelerates the rotating wheel. This motion can be performed from different type of actuators, currently varying in number from 4 to 8 for each wheel.

The most common actuation system on commercial aircraft is hydraulic: the hydraulic energy produced by a pressurized fluid is converted in mechanical energy by the actuator. The pilot input is transmitted to a hydraulic servo-valve by an electric bus, with the fly-by-wire system. This valve (**Figure 3.3**) commonly consists in an electric torque motor that move a flapper, which is the first stage of the valve. The displacement of the flapper, even if very small, produces an asymmetry in the oil flow coming out from the nozzles; this induces a difference in pressure between the two compartments of the valve, generating a displacement of the spool. The pressurized oil, passing through small orifices, flows inside the piston causing the movement. The spool position is fed back to the flapper mechanically through the feedback spring.

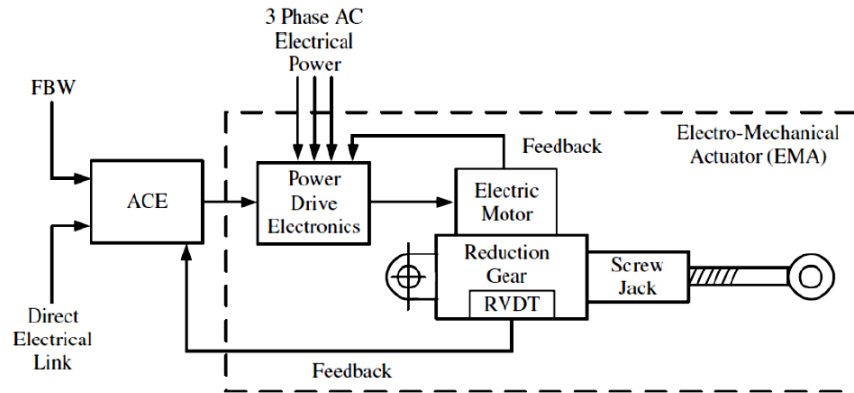


Figure 3.4: Scheme of an EMA servo-actuator ^[23]

In order to replace the traditional hydraulic actuators, another configuration applicable in more-electric aircraft is the *Electro-Hydrostatic Actuator* (EHA), as shown in **Figure 3.5**. The EHA is commonly characterized by an electrically powered system, where a variable speed brushless motor drives a fixed displacement axial piston pump. Pressurized hydraulic fluid then moves a piston in the same way of a classical electro-hydraulic actuators. The circuit is then completed by the presence of:

- Pressure relief valves, with the main purpose to limit the maximum supply pressure;
- Proportional-directional control valve, that adjusts the circuit pressure;
- Small fluid reservoirs.

The actual position of the piston is commonly measured by a *Linear Variable Differential Transducer* and fed back to the control electronics. The advantage of using the EHA is the absence of the centralized hydraulic system that feeds the actuator elements, which is replaced with the electrical system. All the actuator elements are therefore positioned in the point where their use is required. Besides, this system can provide very high forces, exhibits rapid responses and has a high power-to-weight ratio, compared to the previous technologies. All these aspects make them particularly useful in the braking system, where fast actuation forces are required in short time. Actually, these actuators are applied in Primary Flight Control System (especially in light controls). However, thanks to optimization studies and analysis like the ones shown in this thesis, they could be used also in aircraft brake systems.

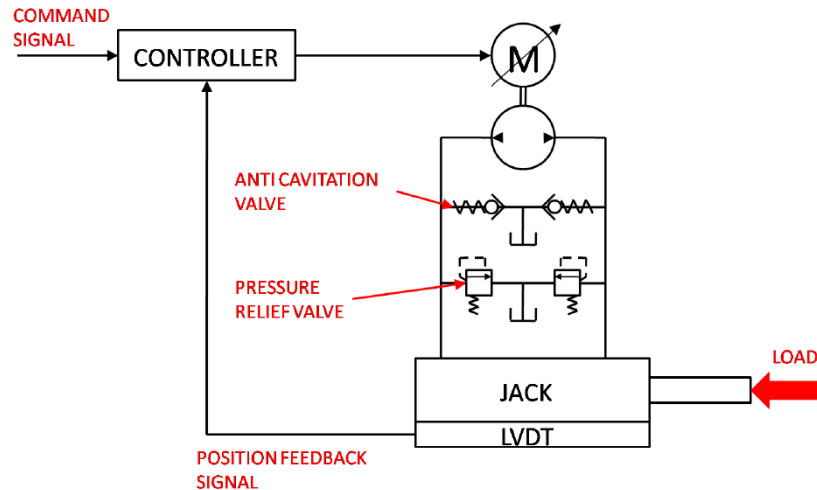


Figure 3.5: Scheme of an EHA [23]

3.2 Architecture Definition

The preliminary design is a fundamental stage in every design cycle, especially for preliminary size, modelling, optimization and features synthesis of system components. Supported by advanced computational tools, early verification and virtual validation of solutions in preliminary design can offer significantly costs reduction and quality enhancement over the entire design process.

The first important step in the design process is the definition of a preliminary architecture, based on a series of system requirements. It consists in drafting a series of potential components and a basic idea as to what their interconnections and functions are. As described above, the braking system of a landing gear needs the wheels and brakes, which are further decomposed into their components including the rolling stock, the actuators, the control units and all the fittings and structural elements. Since these components can interact differently depending on the design choices, a multitude of potential architectures are generated, not all of them feasible. Therefore, it becomes essential to concentrate only on the best candidates inside the design space for future analysis and studies, to avoid high computational costs. To do this, Garcia Garriga A. et al. [24][26] propose a 3-step procedure:

- *Architecture Exploration*, where the architecture design space is explored in order to find feasible architectures;
- *Architecture Evaluation*, where these architectures are evaluated in term of impacts at the A/C level;
- *Architecture Localization*, where the results of the evaluation are processed to find a subset of candidate architectures that can be analysed in more detail at the system level.

For sake of completeness, these three steps are described in the following **Sections 3.2.1, 3.2.2 and 3.2.3**. This overview of the methods proposed by Garcia Garriga A. et al, [\[24\]](#)[\[26\]](#) is intended to give a clear view how the design toolchain related to MISSION is leveraged and how the models developed in the context of this thesis (**Section 3.4**) are employed for the design or system architectures. It must be noted that the models used in such analysis are abstractions of detailed models or existing legacy models. This is presented here to motivate the reader about the applicability of dynamic models developed, upstream in architecture definition phase which is usually an iterative process.

3.2.1 Architecture Exploration

The Architecture Exploration step identifies a feasible collection of architectures excluding all those that violate the requirements defined by the stakeholders and the constraints imposed by regulations. In MISSION, all this process is made by a particular in-house tool called *Architecture Exploration and Enumeration/Evaluation* (AEE) [\[25\]](#). This method follows a filtering process, where the design space is reduced in successive refinement levels. In particular, the method generates an abstraction of the architecture space to rapidly explore it and identify feasible and infeasible solutions. The feasible set is then further screened using higher fidelity analysis in the second step, which is the evaluation phase. **Figure 3.6** shows the AEE technology screening process.

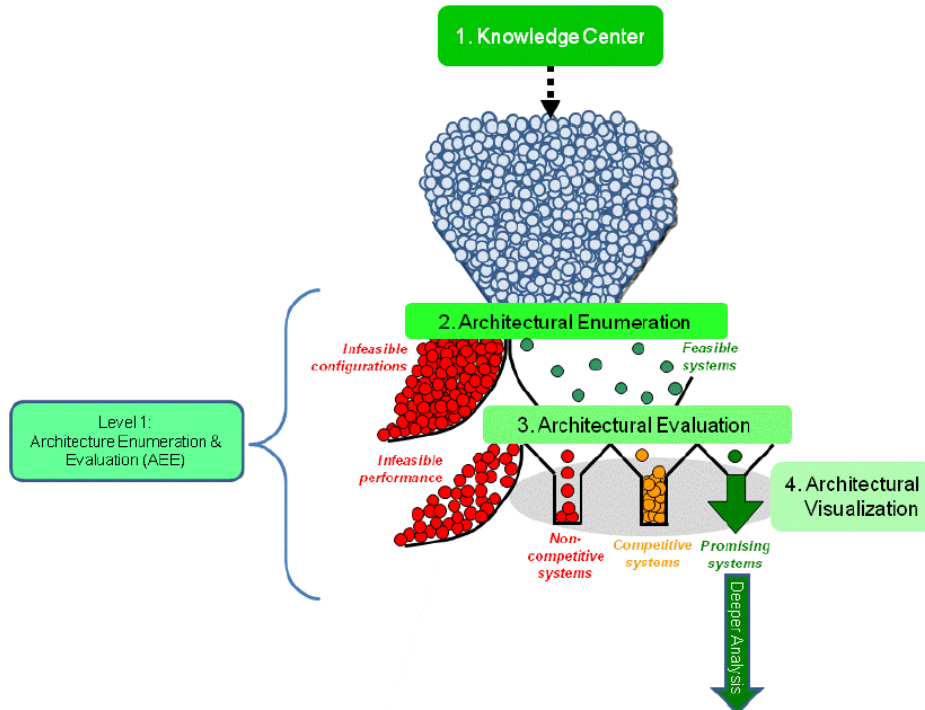


Figure 3.6: Illustration of the AEE method [\[25\]](#)

In order to give a clear view how the method is carried out, the following sections illustrate an application example. The method is adopted to select between two different actuation technologies (electric or hydraulic) for the PFCS of a short range single aisle aircraft, like the Airbus A320 [\[55\]](#). Some preliminary results have been also evaluated internally in UTRC-I for the same actuation configurations, but applied in the landing gear brake system.

The configuration studied [\[24\]](#) [\[26\]](#) on A320 is characterized by:

- Aileron actuators (2 surfaces and 2 actuators per surface).
- Elevator actuators (2 surfaces and 2 actuators per surface).
- Rudder actuators (1 surface and 3 actuators).

Assuming to consider 3 different design options (EHA, SHA or EMA) for each actuator, the number of possible architectures is about 3^{11} . Obviously, many of these potential candidate architectures are not feasible or violate regulatory norms. Typical constraints such as those proposed by Bauer et al. [\[56\]](#) are listed below:

- The left and right aileron and elevator must be exactly symmetrical.
- Each actuator must be connected to the appropriate power source type. For instance, a SHA must be connected to a hydraulic power source; an EMA must be connected to an electric power source.
- Depending on the actuators in the architecture, an appropriate power source (hydraulic and/or electric) must be generated.

- Each actuator must be connected to at least one FCC and to a maximum of two FCCs.
- Each actuator must be connected to only one control surface.
- The actuators for each primary flight control surface must be of (at least) 2 different types.

These constraints serve as the first refinement level in the AEE method and allow to reduce the dimension of the design space by approximately 3 orders of magnitude. In order to explore the design space following some performance and non-performance criteria, it becomes fundamental therefore to develop performance models associated with a specific architecture.

3.2.2 *Architecture Evaluation*

The second step of the method consists to evaluate the impacts at aircraft level of the reduced number of feasible architectures. This process is made using the *power platform process* developed under MISSION project and presented by Garcia Garriga A. et al [\[24\]](#) [\[26\]](#). This application is illustrated just from a descriptive point of view, since it is not part of the work done for this thesis. Nevertheless, the physics-based models developed and presented in this work in the following section could be integrated and tested in such framework with different levels fidelity.

The primary scope of the power platform, developed at UTRC, is to enable trade-off analysis of different aircraft system architectures with respect to some A/C level power objectives. A scheme of the methodology for the power platform design is shown in **Figure 3.7**. The inputs of the power platform are the external requirements, a given aircraft platform and a set of design options and available choices. All these data are fed into different system models represented by dashed blocks. These models, defined a different level of details, have two kinds of outputs: aircraft level impacts (in terms of mass, fuel burn etc.) and their impacts on other systems. In order to reduce the computational cost, these detailed models are run offline or using reduced order surrogates in the first evaluation loop considering as input parameters based on expert knowledge or previous design history. For the case of the PFCS, the models are integrated as power consuming systems and run offline for the exploration step.

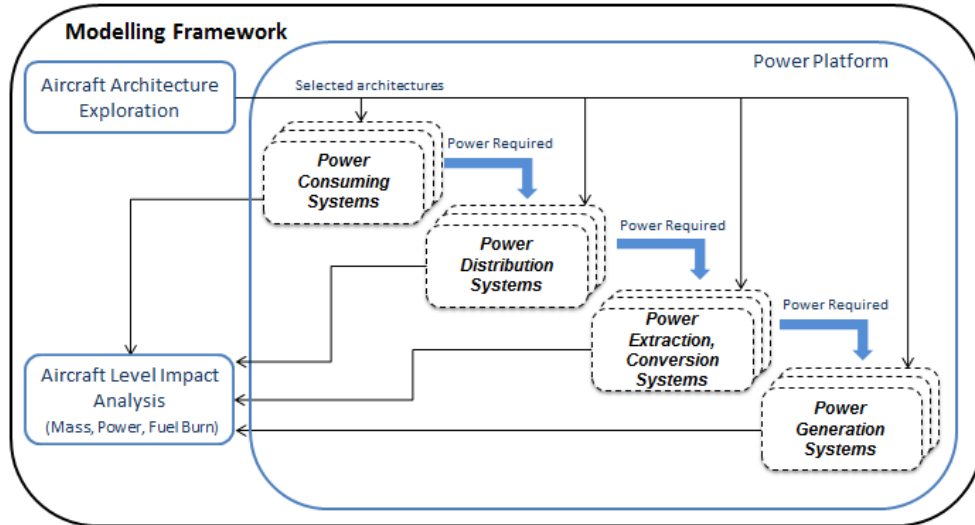


Figure 3.7: Schematic of the power platform data flow [24] [26]

In the study case presented by Garcia Garriga A. et al [24] [26] the dynamic models are developed to be tested in the worst cases scenario, considering the maximum hinge moment and maximum deflection of the surfaces. This will define consequently the size, the geometry and the power consumption of the actuators. All the feasible architecture performances are compared to a baseline conventional aircraft configuration including an all-hydraulic actuation configuration and other conventional systems. The comparison between EHA and EMA actuators and the baseline performance (which is obtained from running the models for each control surface under the same stall load conditions) is presented in **Figure 3.8**. In particular, the power consumed by the electric actuators is compared to the SHA performance, by calculating the hydraulic power needed from the mass flow rate and pressure of the system. From **Figure 3.8** it is possible to notice how both the electric configurations of the actuators are significantly heavier than the conventional hydraulic solution. The diagram shows also how the use of EMA and EHA actuators involves a notable reduction of the power consumption. However, the option with the best performance cannot be established since the lower power consumption of these configurations might balance out their larger mass. Therefore, the need to analyse the effects this change in technology at A/C level becomes apparent early in design process.

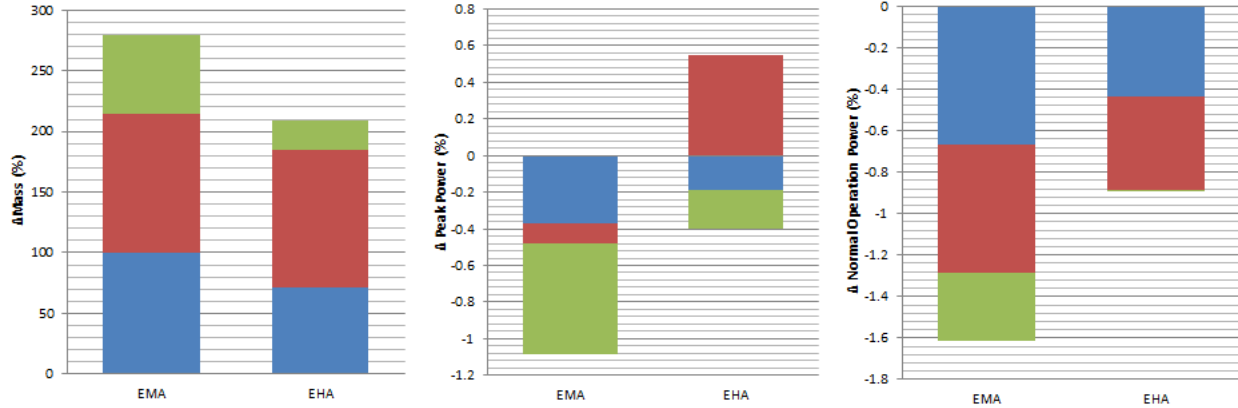


Figure 3.8: Comparison of electric actuator to the baseline [24]

3.2.3 Architecture Localization

In the last step of the method, similar architectures (according to their performances) are grouped into a set of possible solutions, thanks to a clustering algorithm developed internally in UTRC-I and proposed by Garcia Garriga A. et al. [24][26]. The algorithm goes to reduce the number of solution candidates to the cluster centroids, that do not necessarily represent real architectures in the design space. Therefore, it is necessary to refine the selection to a real set of architectures and then, run another discrete optimization loop inside each of the cluster. The performances in term of power extracted, weight and fuel burn are illustrated in the graphs referring to **Figure 3.9**, where each control surface is powered by both hydraulic and electric actuators through hybrid architectures. From the graphs it is possible to notice how the hybrid architecture with EHA's and EMA's is efficient in terms of power required, but heavier compared to the baseline according to what is shown in **Figure 3.8**. This is due to the greater mass of the actuator themselves, that impacts therefore on the overall systems weight.

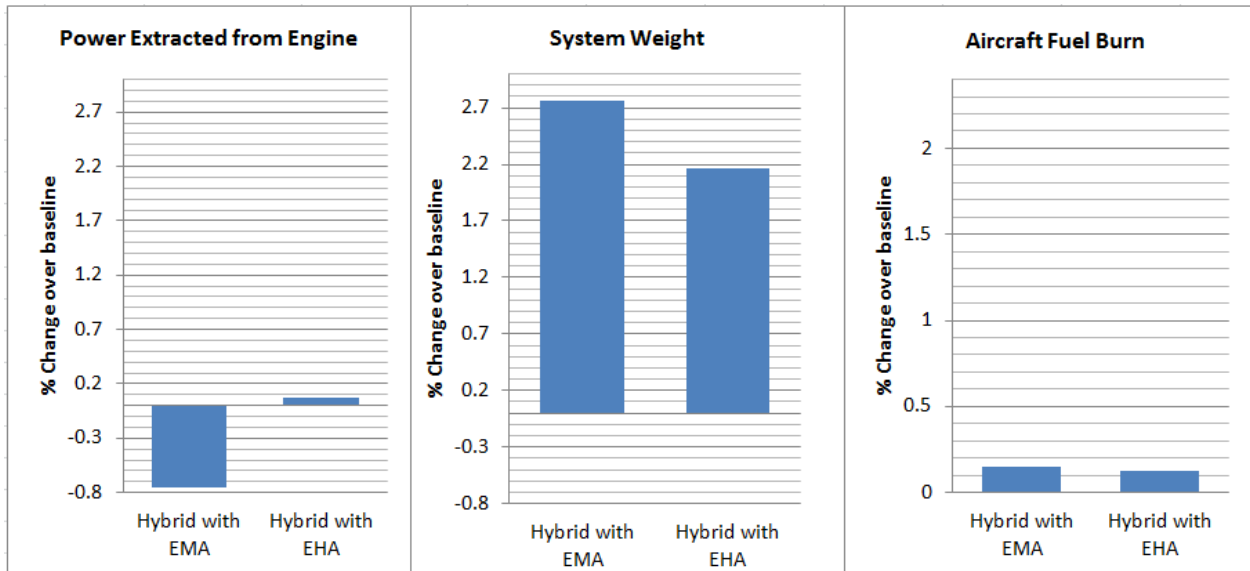


Figure 3.9: Comparison of hybrid architectures with distributed hydraulic and electric power [24]

The primary objective of the work presented by Garcia Garriga A. et al [24] [26] is to define a methodological framework for the trade-off analysis of early design decisions (especially for the PFCS), evaluating a range of possible and feasible architectures according to their performances. Within this context, the models illustrated in this work could be particularly useful.

3.3 System Sizing

This section describes the design process of the brake actuation system and the development of sizing models and their usage in the design optimisation workflow. System sizing is usually the first step in modelling activities, because it is fundamental at this level of the multi-objective design process to obtain low fidelity estimates of system parameters useful for future model simulations and optimization analysis. These data are basically determined by expert designers relying on the historical knowledge or through detailed analyses such as finite element methods for structural or aerodynamic studies based on CAD diagrams and CFD studies.

The approach presented in this work aims to help the preliminary design on the development of models called *estimation models* (or sizing models) that assess the component characteristics requested for their selection before requiring a detailed design analysis. These models enable to obtain design specifications such as cylinder mass, pump displacement, motor speed, motor torque that are then passed as dependent parameters to simulation models. In addition, this

approach to modelling can support a more general methodology capable to capture and incorporate higher fidelity information (for example provided by refined FEM/CAD representations) during all the phases of the design process.

In this document, a sizing model of the landing gear brake systems is proposed. In particular, this model is implemented as a simple MATLAB scripts based on a logical flow that is illustrated in **Figure 3.10**. Starting from generic system requirements and assumptions, it is possible to define a-priori the aircraft architecture, the operational environment and the characteristics of the brake. In particular, the configuration of the A320 has been chosen, including geometry information such as wheelbase, maximum take-off weight and speeds (V_I , V_{taxi} , $V_{landing}$, V_{tyre}). Other inputs include:

- The environment, i.e. the characteristics of the runway (length, width, elevation) and the external temperature;
- The wheels and brakes features, such as the material, the dimensions and friction parameters. In particular, the tire data is referred to the *Michelin* database [\[27\]](#).



Figure 3.10: System sizing logical flow

One of the most important input for both the brake and the actuator system sizing is the aircraft *maximum kinetic energy* (KE) that to overcome by braking. This value is obtained knowing the *A/C mass* ($m_{A/C}$) and the *A/C ground speed* according to **Equation 3.1**.

$$KE = \frac{1}{2} m_{A/C} \cdot V_1^2 \quad (3.1)$$

In this case, the kinetic energy is calculated referring to the *take-off decision speed* V_I , or rather the maximum speed in the take-off at which the pilot must take the first action (e.g., apply brakes, reduce thrust, deploy speed brakes) to stop the airplane within the accelerate-stop distance [\[28\]](#). The choice of this speed has been made considering the brake sizing for the worst scenario, specifically the reject take-off (RTO). Since the kinetic energy is converted to *friction energy* (W_f) according to **Equation 3.2**, the *total longitudinal braking force required* ($F_{Tot,Brk}$) is defined knowing the *stop distance* of the airplane (d_{stop}), which is normally evaluated according to regulations.

$$KE = W_f \quad (3.2)$$

$$F_{Tot_Brk} = \frac{W_f}{d_{stop}} \quad (3.3)$$

By dividing the total *longitudinal braking force* (F_{Tot_Brk}) by the *number of wheels* (n_{wheel}) (it is considered that each wheel has a brake), it is possible to evaluate the *braking force* for each brake (F_{Brk}).

$$F_{Brk} = \frac{F_{Tot_Brk}}{n_{wheel}} \quad (3.4)$$

The *actuator force* (F_0) is then computed following **Equation 3.5**, knowing the *number of actuators* (n_{act}) for each wheel (in this case 4 actuators have been considered) and the *friction coefficient* (μ_{fr}).

$$F_0 = \frac{F_{Brk}}{n_{act} \cdot \mu_{fr}} \quad (3.5)$$

At this point it is possible to size the actuator. The entire sizing sequence can be schematized as shown in **Figure 3.11**, especially for the EHA actuator. In the MATLAB scripts that characterized the sizing model, two different methods are defined to estimate single parameters. The next sections explain in detail the two approaches.

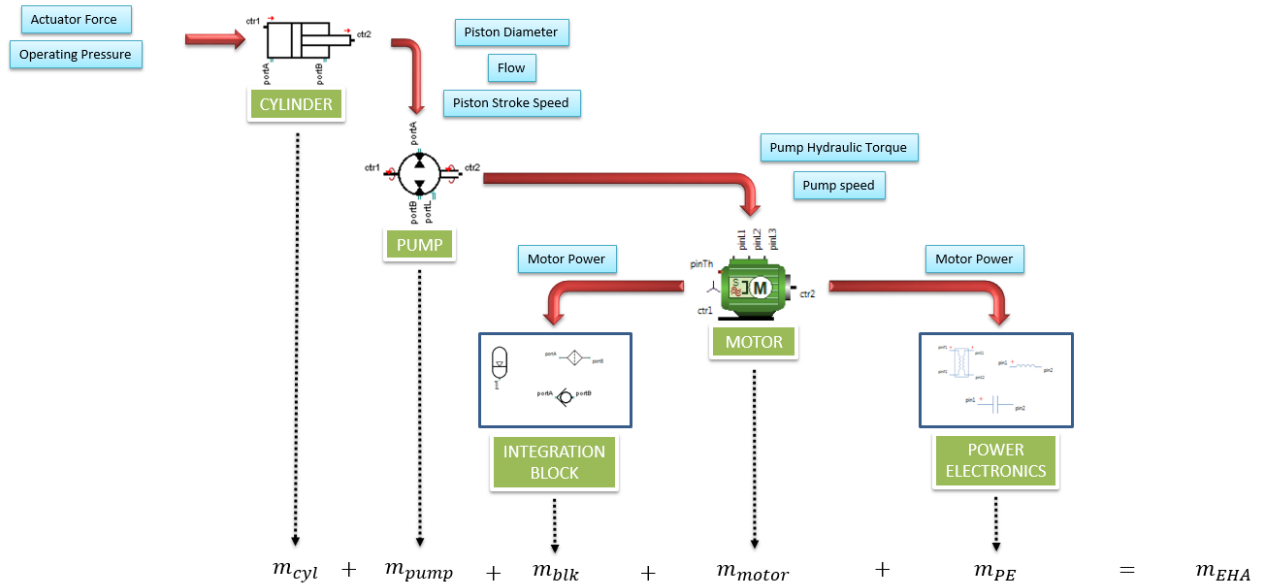


Figure 3.11: Logical flow of the EHA sizing process

3.3.1 Classical Method

The first method is based on available literature component catalogue data to size the actuator cylinder (such as the rod, the piston, the housing volume), then the pump (the displacement and the rotational speed) followed by the motor characteristics (the torque and the speed). In particular, all the mass parameters referring to the *pump* (m_{pump}), the *motor* (m_{motor}), the *power electronics* (m_{PE}) (including capacitors, resistors and so on) and the *integration block* (m_{blk}) (including checking valves, filters, and accumulators) have been predicted by *scaling laws*, according to the relations reported by Wu S. et al [29].

$$\begin{cases} m_{pump} = a \cdot D_m + b \\ m_{motor} = a \cdot T_m^{3/3.5} + b \\ m_{PE} = \frac{P_{motor}}{a} \end{cases} \quad (3.6)$$

$$\{m_{blk} = c_1 \cdot P_{motor} + c_2 \quad (3.7)$$

where a , b , c_1 and c_2 are coefficients given by regression fit of available data and reported in the paper [29], D_m and T_m are respectively the *pump displacement* and the *pump hydraulic torque* and P_{motor} is the *electric motor power*.

The logical steps for sizing the EHA components are:

1. From the max braking load (or else the required actuator force) multiplied by a safety factor (to account for uncertainties) and knowing the operating pressure rating, find the area of jack.
2. Find the rod diameter from catalogue [30] as a function of the braking load and the piston stroke.
3. Find the volume of the piston and its mass.
4. From the tensile yield stress of the cylinder, find the thickness and then the volume of cylinder housing (considering a steel cylinder) and the fluid inside.
5. Find the mass of the cylinder like sum of the mass of housing, mass of piston & rod and the mass of fluid.
6. From the stroke speed and the piston area, find the flow required.
7. Find the equivalent pump delivering this flow from catalogue [31] (if several pumps deliver the flow, consider the one with the smallest displacement subject to speed constraints).
8. Find the pump speed and the hydraulic torque, knowing the hydraulic efficiency (due to the pressure drop).
9. Find the pump mass as a function of the displacement.
10. From the pump parameters, find the electric motor speed and torque.
11. Find the mass of motor as a function of the torque.
12. From the motor characteristics, find the motor power (knowing the motor efficiency).
13. Find the mass of the power electronics as a function of the motor power.
14. Find the mass of the integration block as a function of the motor power.

3.3.2 Similarity Law Method

The second method presents two substantial differences with respect to the previous case. The first difference is in the calculation of the rod diameter, which is obtained with a structural approach based on the buckling load. The *critical load* F_0 , coinciding with the max braking force, is evaluated by the *Euler's equation* (**Equation 3.8**) and the *Rankine's formula* (**Equation 3.9**).

$$F_{0(Euler)} = \frac{c \cdot \pi^2 \cdot E \cdot I}{l^2} \quad (3.8)$$

$$F_{0(Rankine)} = \frac{E \cdot A}{1 + a \left(\frac{l}{k} \right)} \quad (3.9)$$

where c coincides with the *factor* accounting for the *end conditions* (fixed to 4 considering both ends fixed), E is the *modulus of elasticity*, $I = \frac{\pi \cdot d^4}{64}$ is the *moment of inertia* (with d the *rod diameter*), l represents the *stroke*, $A = \frac{\pi}{4} d^2$ is the *piston area*, $k = \sqrt{\frac{l}{A}}$ defines the *radius of gyration* and a is the *Rankin's constant* (it depends on the piston material. Fixed to $a = \frac{1}{7500}$ considering steel). Knowing the geometric and structural parameters, the *rod diameter* d is evaluated as the maximum between the results of the two previous inverted formulae.

The second difference is associated with the definition of the electric motor characteristics related to the actuator: they are evaluated with the use of *similarity laws* presented by Budinger M. [33]. With this approach, the design of the motor requires the definition of a significant number of parameters and the estimation of changes for these ones compared to an existing/reference component. For doing that, two constraints must be imposed:

- *Material similarity*: all material and physical properties are assumed to be identical to those of the reference component;
- *Geometry similarity*: the ratio of all the lengths of the component under consideration to all the lengths of the reference component is constant.

The similarity laws are implemented in a MATLAB script, dedicated to motor sizing; **Table 3.1** reports the laws with the reference on a *PARVEX NK-420* electric motor.

Table 3.1: Similarity laws of motor parameters [\[33\]](#)

PARAMETER	SIMILARITY LAWS	UNIT
MOTOR DIAMETER	$d_m = d_{m_ref} \cdot \left(\frac{T}{T_{ref}}\right)^{1/3.5}$	N·m
MOTOR LENGTH	$l_m = l_{m_ref} \cdot \left(\frac{T}{T_{ref}}\right)^{1/3.5}$	m
MOTOR MASS	$M_m = M_{m_ref} \cdot \left(\frac{T}{T_{ref}}\right)^{3/3.5}$	kg
BUS VOLTAGE	$V_{BUS} = V_{BUS_ref}$	V
SATURATION CURRENT	$i_{sat} = i_{sat_ref} \cdot \left(\frac{T}{T_{ref}}\right)^{2.5/3.5}$	A
MOTOR INERTIA	$I_m = I_{m_ref} \cdot \left(\frac{T}{T_{ref}}\right)^{5/3.5}$	kg·m ²
COPPER-IRON RESISTANCE	$R_{CI} = R_{CI_ref} \cdot \left(\frac{T}{T_{ref}}\right)^{-2/3.5}$	k/W
COPPER CAPACITY	$C_C = C_{C_ref} \cdot \left(\frac{T}{T_{ref}}\right)^{3/3.5}$	J/k
IRON CAPACITY	$C_I = C_{I_ref} \cdot \left(\frac{T}{T_{ref}}\right)^{3/3.5}$	J/k
JOULE LOSS COEFFICIENT	$\alpha_m = \alpha_{m_ref} \cdot \left(\frac{T}{T_{ref}}\right)^{-5/3.5}$	W/N·m ²
IRON LOSS COEFFICIENT	$\beta_m = \beta_{m_ref} \cdot dv_l \cdot \left(\frac{T}{T_{ref}}\right)^{3/3.5}$	W/(rad/s) ^{1.5}
MOTOR SPEED	$w_m = w_{m_ref} \cdot \left(\frac{T}{T_{ref}}\right)^{-1/3.5}$	rad/s

For sizing the power electronics and the motor housing, two formulae have been used deriving from *ACTUATION2015* [\[32\]](#) project. In particular, the power electronics mass is calculated as a function of the length, with and depth of the power electronics block and the heatsink mass. The motor housing mass instead is defined in function of the dimensions of the motor housing. Knowing the mass of all the components, the *mass of the EHA* (M_{EHA}) is computed as summation overall the *mass components* (M_i) defined in **Equation 3.10**.

$$M_{EHA} = \sum_{i=1}^N M_i \quad (3.10)$$

where N is the *number of actuator components*. In addition to geometric and performance parameters, thermal characteristics are also estimated according to the relation proposed by Daidzic N. and Shrestha J. [34].

$$T_{brake_r} = \frac{KE}{m_{brake} \cdot c} \quad (3.11)$$

where the *temperature rise* in the brake T_{brake_r} is calculated as function of the kinetic energy KE and the *specific heat capacity* c . Finally, the scripts give also simple estimate of reliability, linked with the number of brake wear cycles (considering 99 % of wear) and the number of possible missions and reject take-offs before replacing the brake. The considering mission scenario is characterized by six stops at 25 knots (three for taxi-out and three for taxi-in with a brake wear of 25 % for each taxi maneuver), plus a landing stop at 195 knots.

Tables 3.2 and 3.3 show a list of the so called *key design drivers*, i.e. the relevant parameters used to size the EHA components and also the results of the sizing process, in term of mass of a single EHA. In both the tables the values associated with the first method have been set as references, while the parameters of the second method have been evaluated as percentage variation of the references (in order to protect the technical data produced internally in UTRC-I).

Table 3.2: Key design drivers values (1)

<i>Parameters</i>	<i>Method 2 Percentage Variation on Method 1</i>	<i>Unit</i>
CYLINDER		
<i>Rod Diameter d_{rod}</i>	- 9.41 %	mm
<i>Mass m_{cyl}</i>	- 2.22 %	kg
ELECTRIC MOTOR		
<i>Mass m_{motor}</i>	- 37.31 %	kg
FULL EHA		
<i>Mass m_{EHA}</i>	+ 9.27 %	kg

From **Table 3.2** it is possible to notice how both the rod diameter (and consequently the mass of the cylinder) and the electric motor mass are decreased comparing the values of the first sizing method. These changes are therefore reflected in different values assumed by the EHA mass at the end of the sizing process. Unlike the other parameters shown in the table, the EHA mass is increased respect to the reference values (+ 9 %). This value is motivated by different

methodology adopted for the calculation of the power electronics mass: adopting the A-2015 method, the mass of this block is increased more than 90 %, causing the increasing of the EHA mass.

In **Table 3.3** instead the percentage variation of the parameters is set to 0 %. This because the key design drivers are evaluated with the same equations in both the sizing methods.

Table 3.3: Key design drivers (2)

<i>Parameters</i>	<i>Method 2 Percentage Variation on Method 1</i>	<i>Unit</i>
CYLINDER		
<i>Max Braking Load $(F_{brk})_{max}$</i>	0 %	kN
<i>Operating Pressure p</i>	0 %	Bar
<i>Piston Diameter d_{piston}</i>	0 %	mm
<i>Piston Stroke $strk$</i>	0 %	mm
<i>Piston Stroke Speed $strk_speed$</i>	0 %	m/s
PUMP		
<i>Required Flow Q</i>	0 %	m ³ /s
<i>Displacement D_m</i>	0 %	ml/rev
<i>Hydraulic Torque T_{hyd}</i>	0 %	N·m
<i>Rotational Speed ω_p</i>	0 %	rpm
<i>Mass m_{pump}</i>	0 %	kg
ELECTRIC MOTOR		
<i>Torque T_m</i>	0 %	N·m
<i>Power P_{motor}</i>	0 %	W

3.4 System Modelling and Simulation

This section illustrates all the modelling activities related to the system design chain. Once the design variables coming from the sizing process are fixed, the second step consists to choose which is the most advantageous tool and the appropriate modelling language to develop models. Then, once model commercial/open libraries have been selected, it is possible to start the model development.

3.4.1 Modelling Tools

All the dynamic models are built upon standardized multi-domain modelling language Modelica, with the use of two different tools: *OpenModelica* and *SimulationX*. The first is an open-source Modelica-based modelling and simulation environment. The software is free distributed in binary and source code form for research, teaching, and industrial usage. In particular, it has been used to learn the physics-based modelling and the a-casual characteristics of Modelica language. The second is a computer-aided engineering proprietary tool used as main simulation environment for all the modelling activities in the MISSION project and for the work discussed in this thesis. The choice of this tool has been made because it represents the “state of art” for modelling and simulation software, able to offer different modelling approaches, including classic dynamic analysis of linear and non-linear systems modelled with equations, to physics based and signal-oriented modelling.

The first modelling approach, known as *network modelling*, is the simplest way to describe any kind of physical behaviour in physical object-oriented modelling activities. The models are developed in terms of *objects* which are interconnected to each other by *connections*, also called *nodes*. In SimulationX, the objects are pre-defined components from various physical domains, whereas the connections are created simply connecting elements to each other at ports. One of the most important characteristic of the network connections is their *bi-directionality* also called *a-causality*. Unlike main simulation tools (Simulink for example) where it is possible only evaluate the effects that the variation of input parameters have on the output, the special connection types of SimulationX allow to transfer the information in both directions. One of the main advantage is that the physical architecture is more or less preserved in modeling.

In SimulationX, the physical relationships in network models are formulated in terms of *potential* and *flow quantities*. The potential quantities reside in a connection and are identical for all element connectors. These are, for example, the displacement, the speed, and the acceleration in mechanics, pressure in fluid libraries, voltage in electronics, or temperature in thermal models. The flow quantities instead are parameters, for which some balance equations must be fulfilled. For instance, forces or torques at connections in mechanics must balance to zero. Knowing therefore the real physical element that must be modelled and his behavior, the

user can easily translate it in a model using the physical model packages, with pre-defined basic and advanced model components.

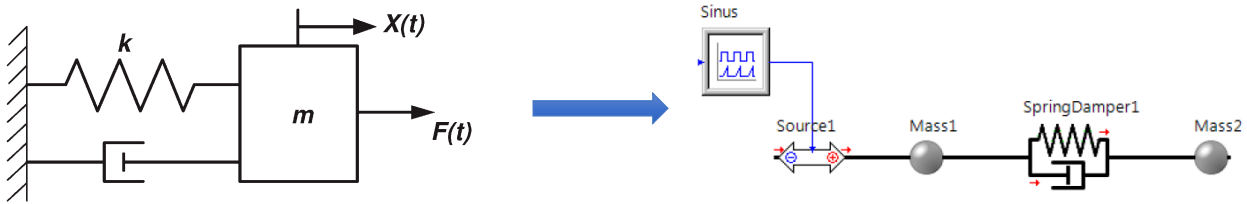


Figure 3.12: Translation between physical model and simulation one

Another approach for modelling is the *signal-oriented*, in which the elements of a signal structure generate output data from input provided to them. In this type of models, it exists a clearly defined information flow and causality. The physical models are connected to the signal-oriented ones thanks sensors, which translate physical quantities into signals. This modelling approach is used to model control systems and auxiliary structures for computing dependencies in physical libraries. An example of a signal-oriented model is shown in **Figure 3.13**.

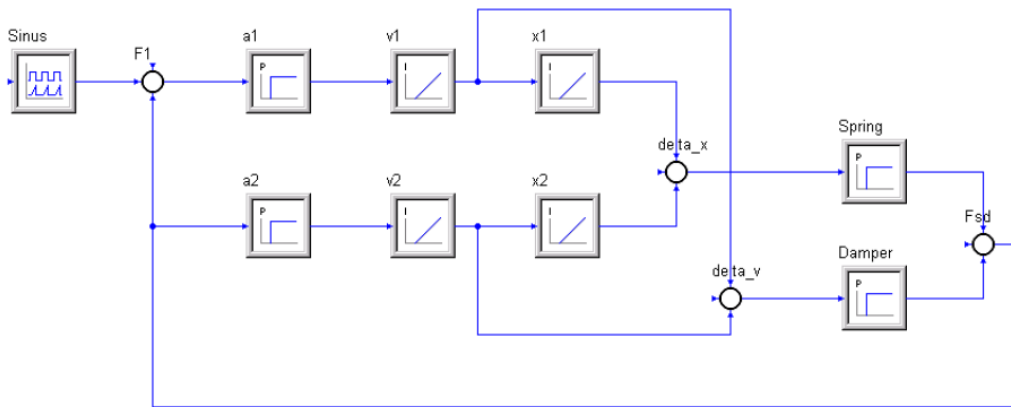


Figure 3.13: Example of signal-oriented model [35]

Another greater advantage offered by SimulationX is to provide interconnections with other common industry-standard tool, using the Functional Mockup Interface standards. FMI is an independent standard tool to support both model exchange and co-simulation of dynamic models, using a combination of xml-files and compiled C-code [4]. Its primary function is to create a component called *Functional Mockup Unit* (FMU) that contain a copy of the binary

code of the developed model. **Figure 3.14** shows the schematic workflow of a FMI (for model exchange) code export.

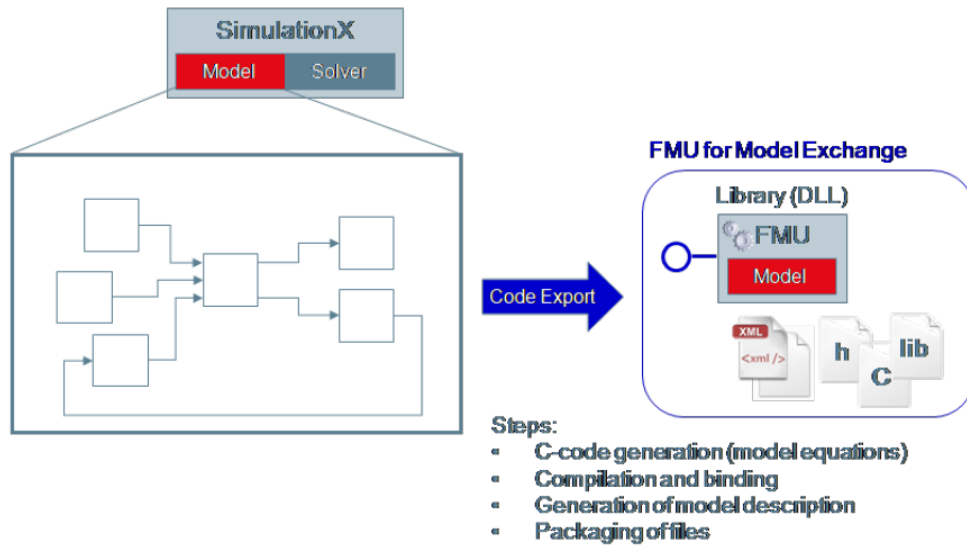


Figure 3.14: FMI Code Export for Model Exchange [\[35\]](#)

Thanks to the FMU, it is possible to reuse and manage the models with different simulation tools and also to protect the intellectual property of the supplier. During the code generation, the model's developer can select which variables and output show to the user and also the type of FMU: if the model contains proprietary information, the tool wraps it in a sort of "black box" such that the user cannot access inside.

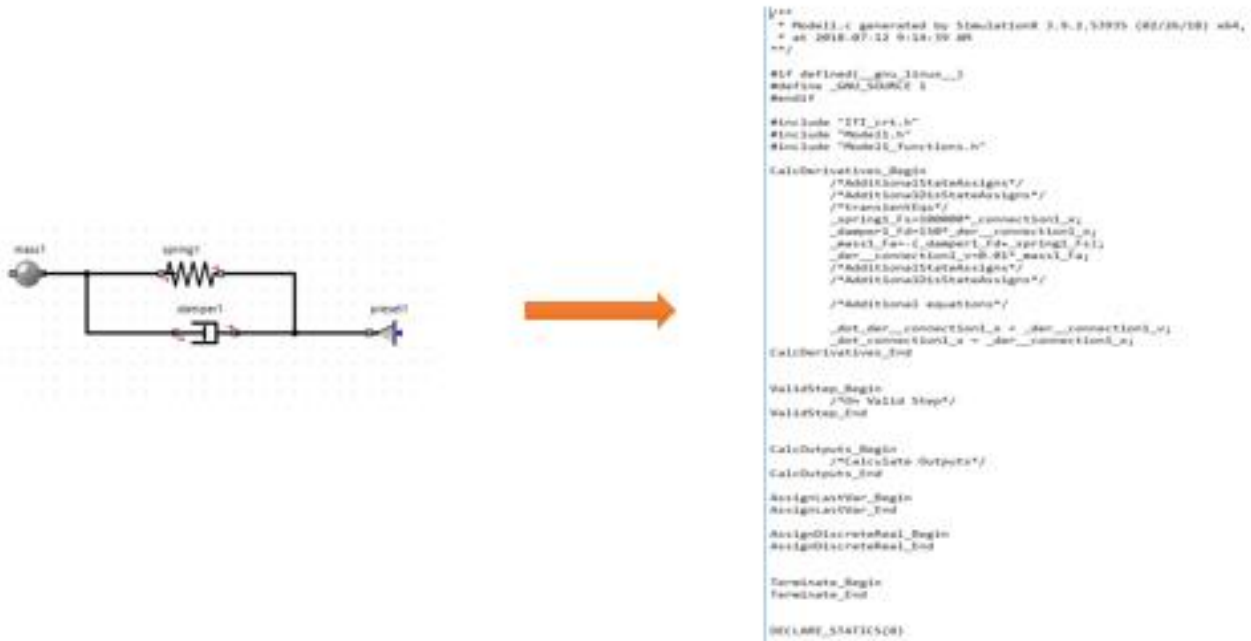


Figure 3.15: Spring-damper oscillator exported as FMU

In Section 3.4.2 some aspects of modelling approach are explained along with application to the modelling problem. This is to illustrate both the process and application.

3.4.2 Hierarchical Modelling

One of the key advantage of using Modelica is the *hierarchical modelling*. This approach is useful because it gives a better overview and clear structure of the developed models and helps with easy maintainability of different fidelity and their usage depending on intended purpose. Some key aspects in system design, combined with the hierarchical modelling approach, are the concepts of *partial models* and *standard interfaces*. A partial model is a kind of empty “black box” which can be filled with different fidelity models, while the interfaces represent the “connections” between the various partial models (i.e. hydraulic, mechanic, electric, thermal). **Figure 3.16** shows a schematization of these concepts. The macro blocks *A* and *B* shown in the figure represent the partial models, which are extended with different fidelity models A_1, A_2, A_3, B_1, B_2 and B_3 . Through the same interfaces, defined by the coloured arrows, it is possible to link the partial models and fill them with the models mentioned above, creating what is called the “hierarchy” between models.

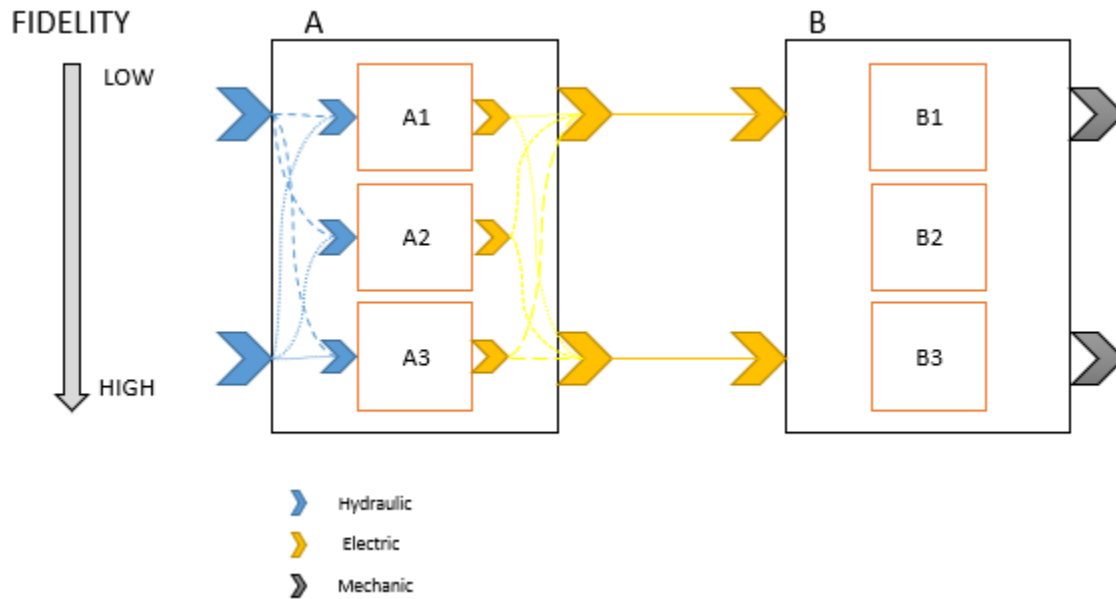


Figure 3.16: Graphical representation of partial models and interfaces

The advantage of this modelling concept is combined with the possibility to fill the empty partial model with any kind of models organized in hierarchical way. Depending on the application, these models can be chosen and connected to each other, as long as the interfaces of the external partial models are respected. For example, if the interfaces of a partial model are electric (as in the case of the block *A* shown in **Figure 3.16**), the parameters referring of the internal models must be of the same type, in order to guarantee the connections.

In SimulationX, the model developers have at their disposal a sophisticated development environment called *TypeDesigner* that allows to create partial models. Thanks to *TypeDesigner*, it is possible to develop user-defined elements specifying connectors, model components, enumerations and documentations.

For the work done in this thesis, the hierarchical modelling approach is applied to create a package similar to a Modelica standard library, in which the user has the possibility to choose between two different types of hydraulic valves:

- The first one is a *4/3 proportional-directional control valve*, which is already inside the SimulationX library in the hydraulic package (which is illustrated in detail in the next section of the document);
- The second is a custom control valve like the one mentioned above, with some extension elements.

The implementation of the two valves is shown in **Figure 3.17**, where they are connected with other elements such as a double acting cylinder, hydraulic lines and pressure sources. The left model shown in **Figure 3.17** represents the custom valve, while the other model is related to the *4/3* control valve. The simple actuator models shown in the figure are not completely

described in detail, because the goal here is to create a partial model and fill it with the two valves models.

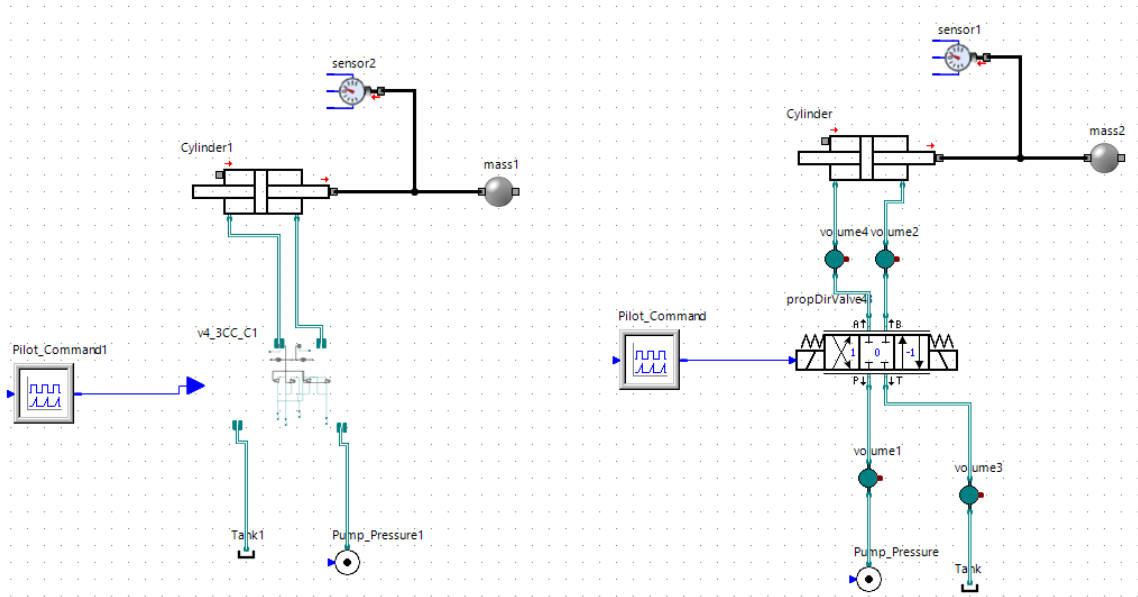


Figure 3.17: Implementation of the two hydraulic valve models

With the reference to **Figure 3.16**, the two valves (coinciding for example with the internal block A_1 and A_2) are inserted in a partial model (the macro block A) and both connected with the external hydraulic connectors (the interfaces). By selecting this partial model and connecting it with the external elements (i.e. the devices that characterize the actuator), it is possible to choose directly from the SimulationX command window which type of valve to use, without intrusively accessing their representations. Once the valve model is chosen, the user must define simply the parameters associated to the selected element, because the hydraulic connections of the other valve presented in the partial model are bypassed.

Figure 3.18 shows the realization of the partial model and its extension with the two valve models described above. However, all the models have been developed so that the user can access inside each component by opening the various compound but cannot modify. **Figure 3.19** shows the internal view of a custom valve, compared with its physical representation. The spring-mass system represents the mechanical part of the 2nd stage of the servo-valve, i.e. the spool displacement. The two elements named as “Area_X” and “Area_Y” (piston area elements in the hydraulic library of SimulationX) are used to model the hydrostatic pressure force acting on the spool surface. For what concerns the four valve edges, they are used to model the flow cross section areas, that is the spool openings where the pressurized oil flows. With these elements, the users can select among several pre-defined geometric shapes or specify directly the function between the opening area and the spool stroke. The high-fidelity model of the

valve represents an extension to a normal 4/3 control valve mode: this configuration takes into consideration not only the hydraulics characteristics, but also the edge's geometry, therefore leading to a higher fidelity model.

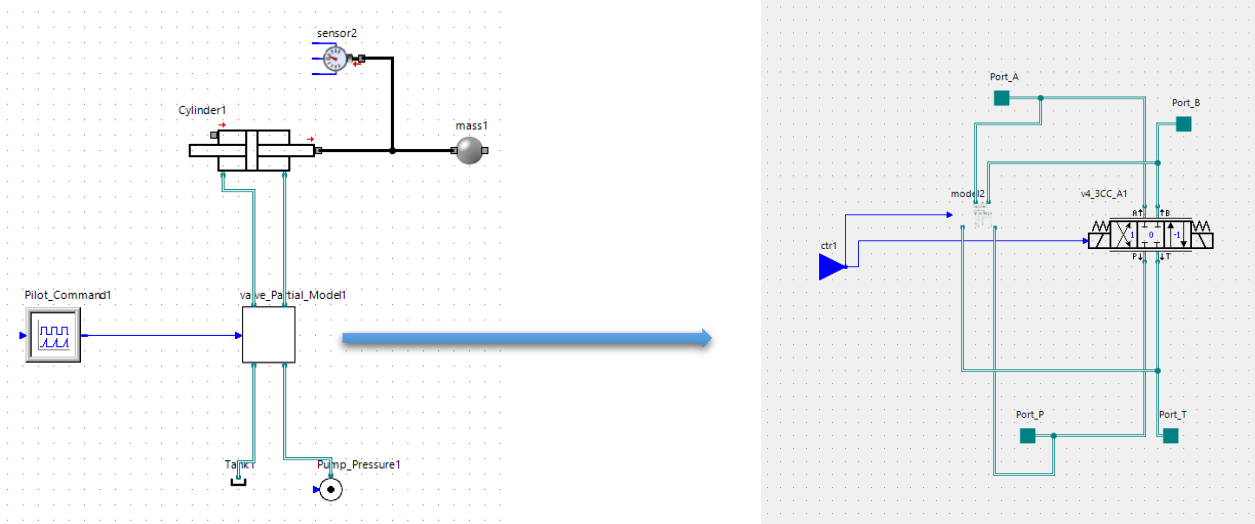


Figure 3.18: External and internal view of the valve partial model

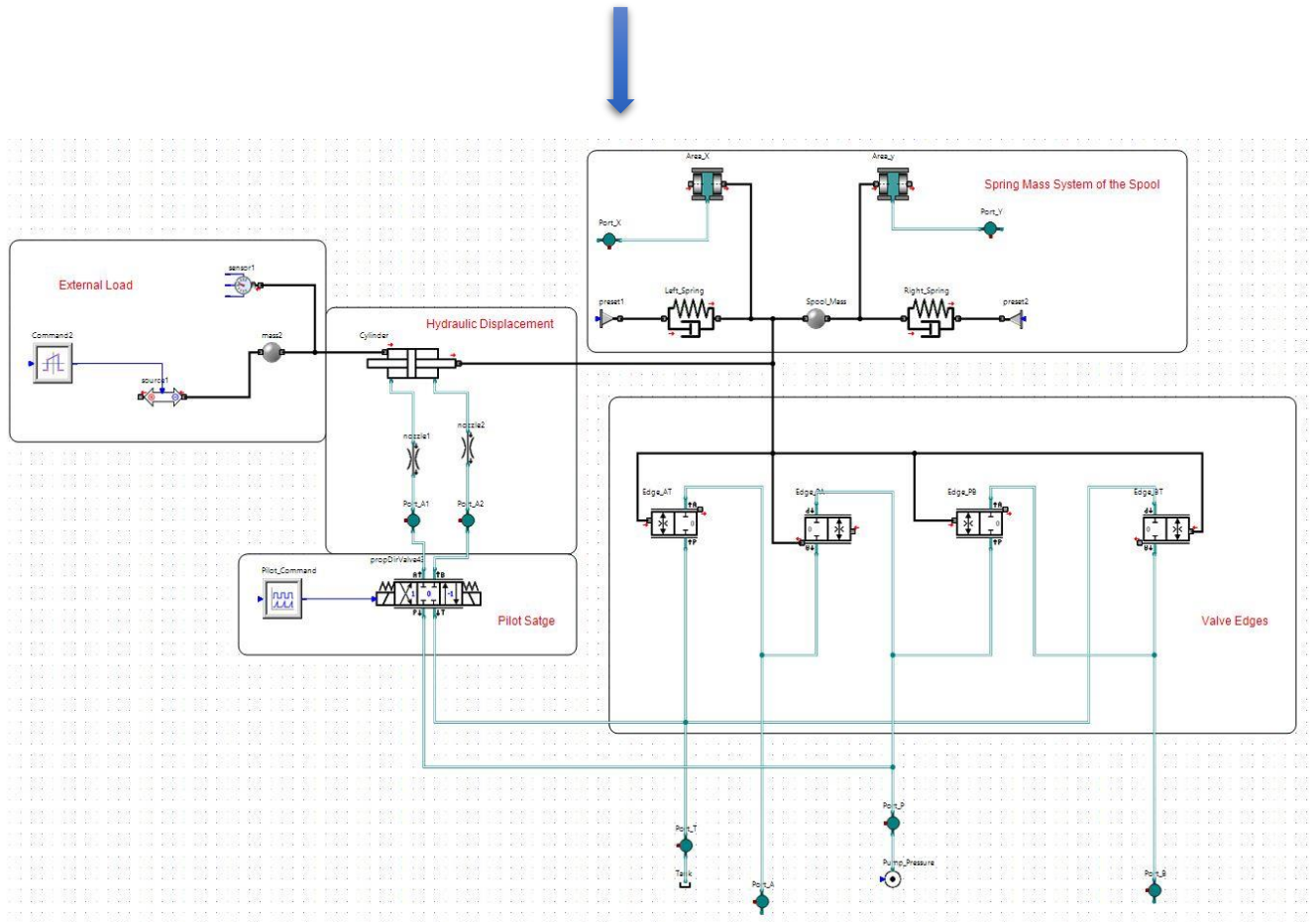
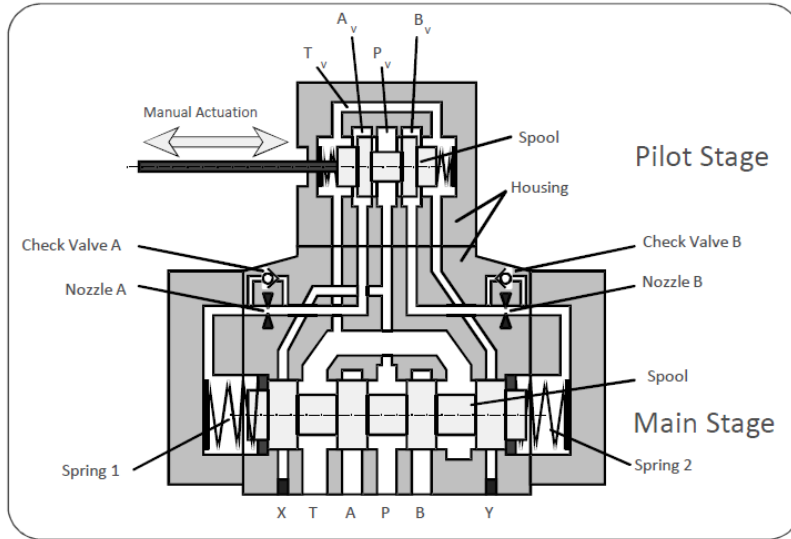


Figure 3.19: Real valve representation (up) [36] and dynamics model (down)

Figure 3.20 shows the piston stroke related to the cylinder (**Figure 3.18**) of the two valves, while **Figure 3.21** the pressure drop; the green line is referred to the model with the default 4/3 valve, whereas the red represents the response of the custom valve. In comparison, the two valves show the same trend except for the initial phase where the dynamic response of the custom valve presents some oscillations, probably caused by the different geometry that distinguishes the two valves.

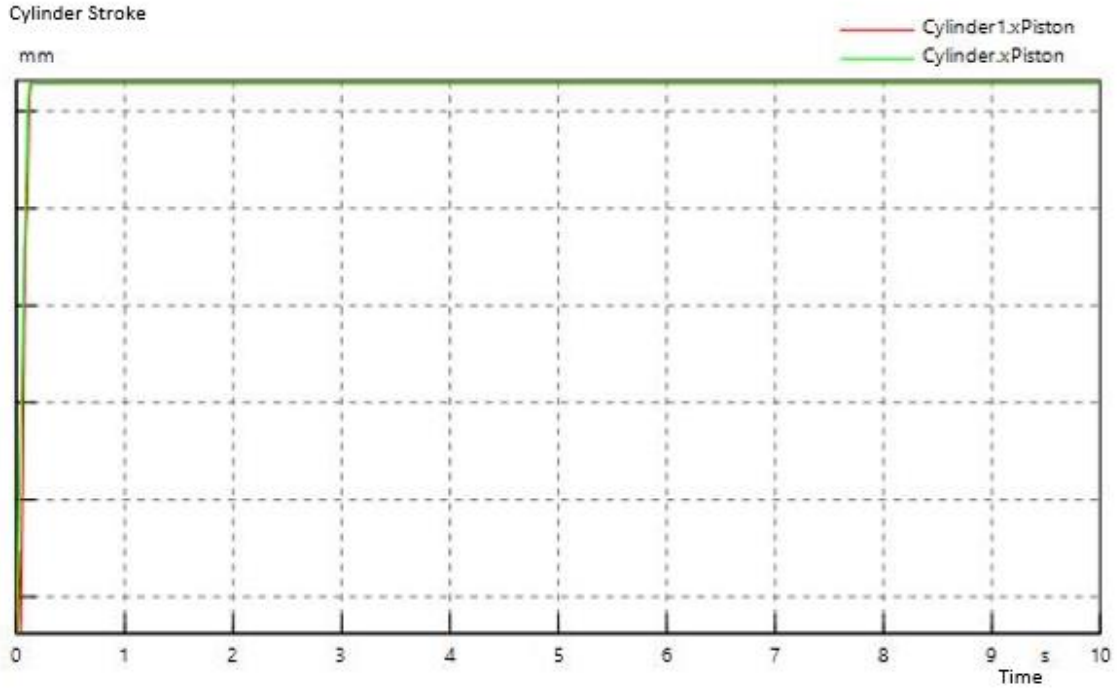


Figure 3.20: Piston stroke of the two valves

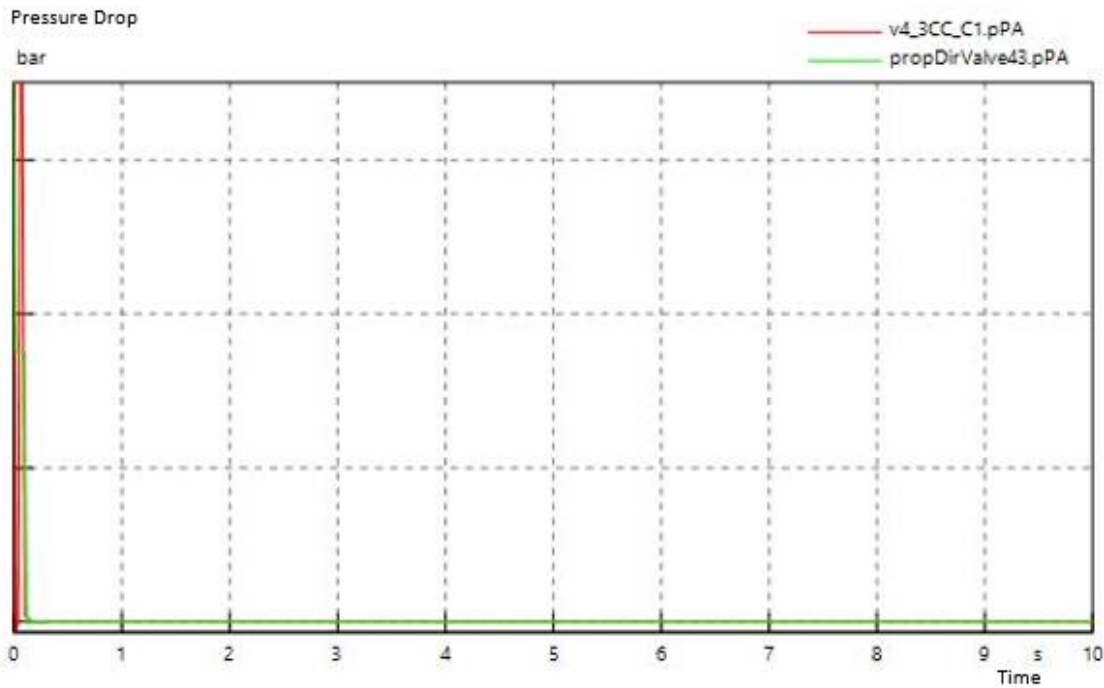


Figure 3.21: Pressure drop of the two valves

3.4.3 Library Comparison

The use of open libraries to realize and compare models often implicates the absence of useful elements to model dynamic behaviors of different complexity. Therefore, it becomes fundamental to make a trade-off and choose between different types of libraries, before starting any modelling activities. The choice is between two options: to develop directly the missing models with an open library, writing the equations with the standard Modelica language; or acquire directly a commercial library that contain inside all the useful elements. Usually, this choice is based on how much a commercial library costs with respect to the man-hours expenses to develop a new one.

The next paragraphs illustrate the different libraries. In particular, a first comparison is made between two model libraries used to realize the electric motor of the actuator. The second comparison instead, is referred to the hydraulic elements of the actuator.

Electric Motor Library

Under some circumstances, it is important to develop new components not available in standard library. A key application of this approach is given by the use of A-2015 library, created under the project ACTUATION2015 [\[32\]](#), for modelling electric motor. This library contains a common set of standardised, modular and scalable EMA models for different uses (flight control, high lift, landing gear, door, thrust reverser) and for all types of aircraft (business/regional/commercial airplanes and helicopters). This library is used to develop an electric motor model shown in **Figure 3.22**, which it is applied then to the various actuator models. The selected motor is generic three phase electrical machine, which is mainly characterized by the *electrical torque constant* K_t , which expresses the relationship between *torque* T_m and *current* I_A .

$$K_t = \frac{T_m}{I_A} \quad (3.12)$$

The control logic is implemented by creating a speed controller, because the motor model is speed controlled. In particular, the controller provides the current loop with the required current based on the feed-back speed, measured by a speed sensor linked to the motor shaft. The speed demand is then passed to a PI controller with a filter upstream that reduces the possible noises come from the input signal. To close the control loop, a 3-phase current controller plus the electric power supply block (comprising a DC voltage source and an inverter) are inserted, to feed the motor with the required current.

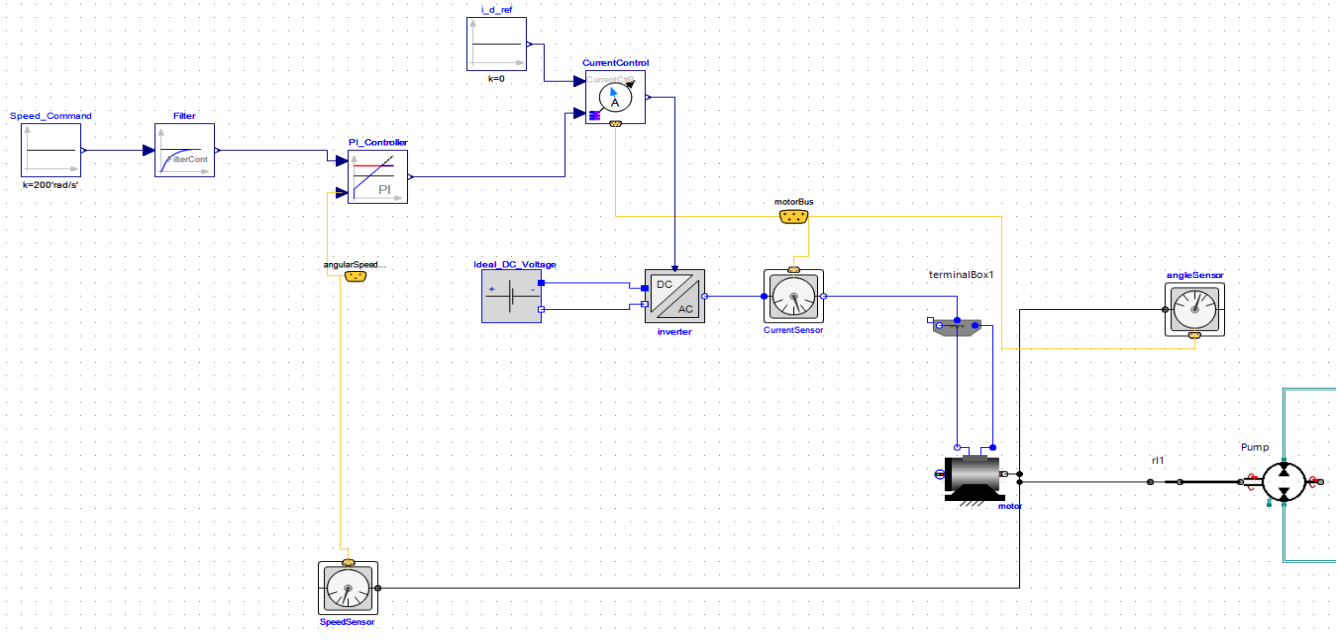


Figure 3.22: Custom electric motor model

This motor model is compared with a *servo-motor* model, comes from the SimulationX proprietary library, in order to decide which type of elements library adopt. This model represents a speed-controlled motor, including the PI controller and current limitation. **Figure 3.23** shows the external representation of the motor model, while **Figure 3.24** shows the internal structure.

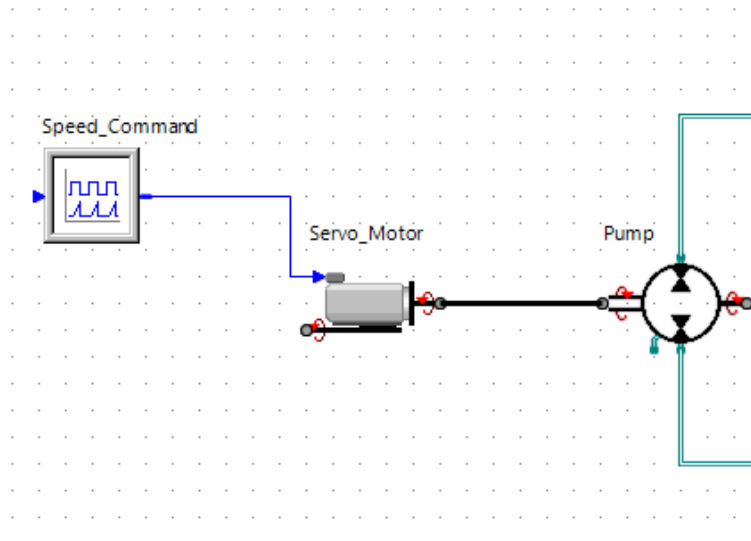


Figure 3.23: Servo-motor application model

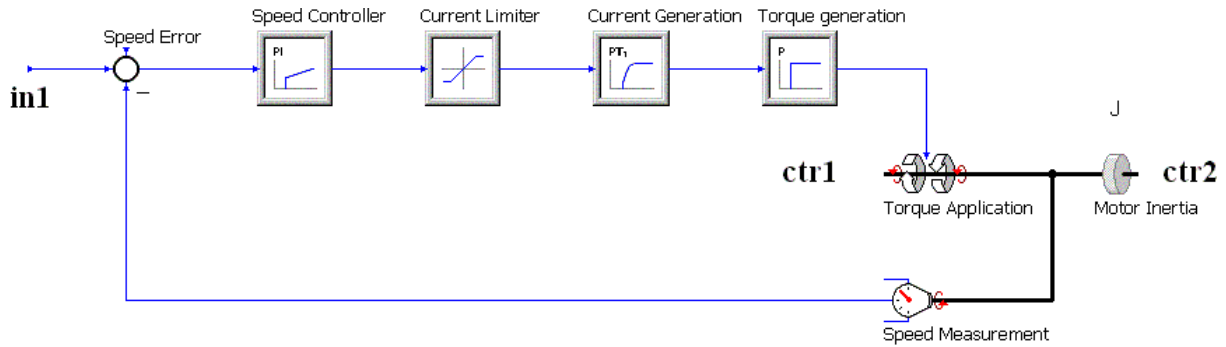


Figure 3.24: Servo-motor internal view [\[35\]](#)

Inserting the same control gains in the controllers and giving the same speed command as input (a constant signal), the dynamic responses of the two models are similar, as shown in **Figures 3.25** and **3.26**. In particular, **Figure 3.25** shows the motor torque of the two models compared, while **Figure 3.26** shows the rotational speed measured by the speed sensor. From this figure it is possible to notice how the motors reach the command speed with a fast response, but the servo-motor shows some oscillations in the settling phase. This discrepancy is probably associated with the different elements involved in the internal structure of the motor models and from the different control logic. Since the trends of the dynamic responses of the two models compared are similar, the choice of a library like the A-2015 is preferable. This because it allows to modify a larger quantity of parameters, by accessing directly into the elements; this indeed, is not possible with a proprietary elements library such the SimulationX one. In addition, its hierarchical nature makes it more applicable for further design optimisation tasks.

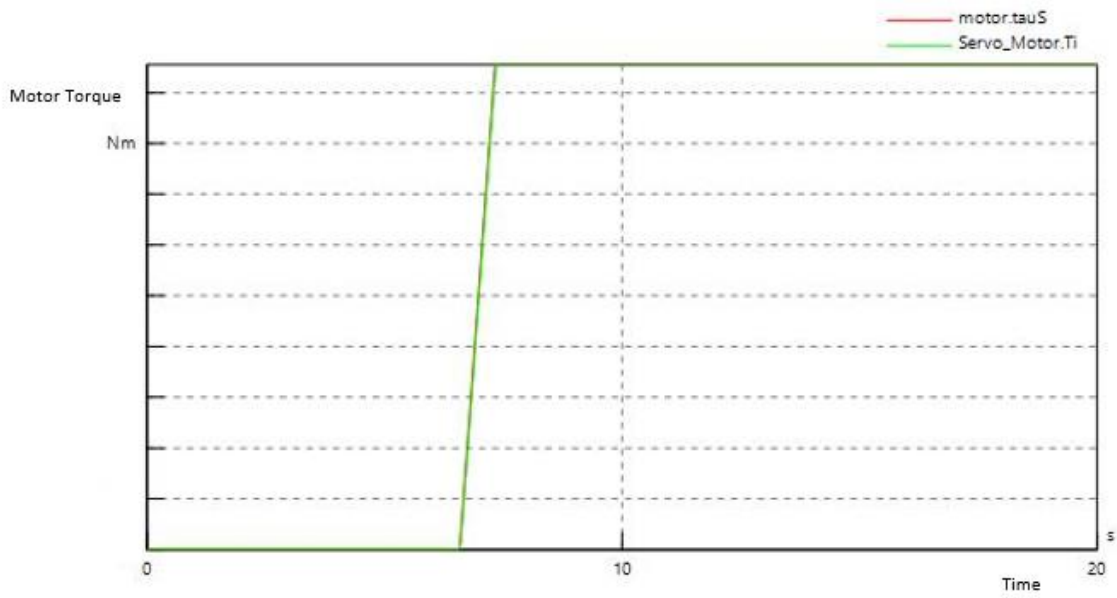


Figure 3.25: Motor torque of the two different motor models

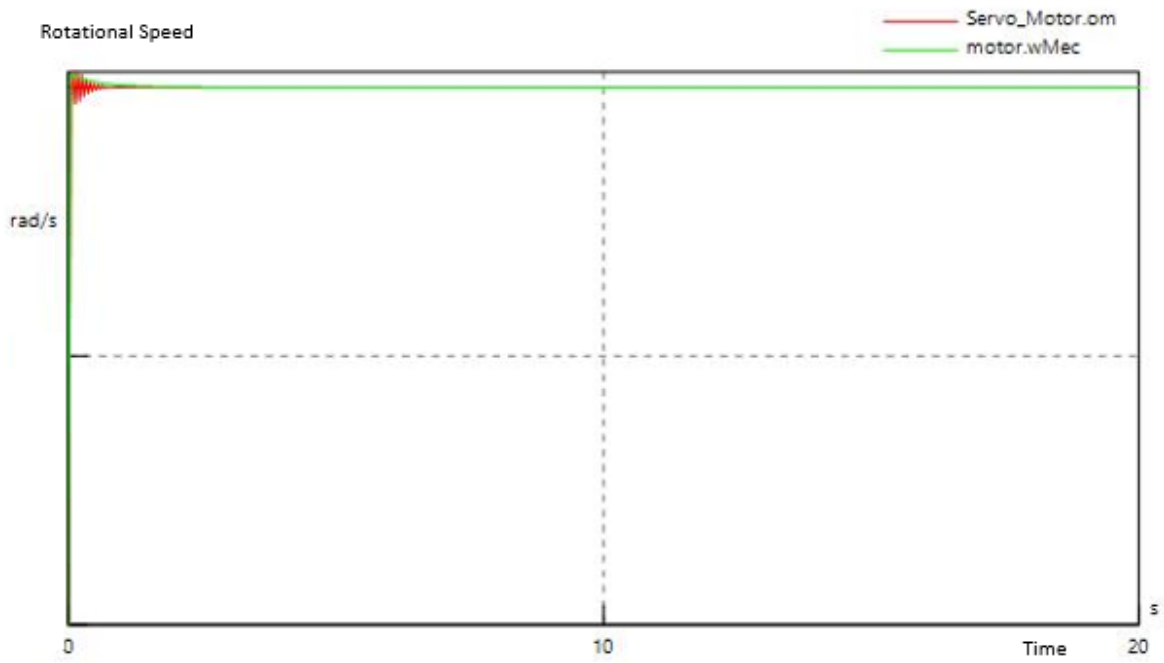


Figure 3.26: Motor shaft speed of the two motor models

Hydraulic Library

For what concern the hydraulic elements of the actuator, the library selection has been made between an open library and a commercial one. To pursue this decision, two simple EHA models are compared focusing only on the hydraulic and mechanical elements, neglecting the electric motor and the motor-drive electronics.

The first model library is *OpenHydraulics* [\[37\]](#), which is a free-standard Modelica package downloadable for free from internet and used to model hydraulic components and circuits. Like all the Modelica libraries, the package is built up in a hierarchical way, starting from basic fluid phenomena such as pressure, volume and temperature sources, laminar restriction etc. These basic models are then combined into models for hydraulic components (cylinders, lines, motors-pumps, sensors, valves, volumes). Finally, these components are incorporated into circuits, such as a pressure compensated load sensing circuit.

The second library instead is presented inside SimulationX environment. Since the developed models are made in a physical-oriented perspective, the users can create models according to the hydraulic circuit diagram, without any need for setting-up differential equations, signal flow diagrams or transfer functions. Furthermore, many elements provide an interface to other domains and libraries. For example, the hydraulic actuators can be connected to elements from the library *Mechanics*, and completed with elements from the *Thermics* library, in order to account for heat transfer effects. **Figure 3.27** shows the structure of the two hydraulic libraries (the left library is OpenHydraulics, while the right library is the SimulationX one).



Figure 3.27: Draft of OpenHydraulic (left) and SimulationX (right) libraries

Figure 3.28 shows the EHA model realized with OpenHydraulics. For what concern the one developed with SimulationX components and realized by one of the UTC business unit, a detailed description of the involved elements will be provided without the insertion of any images, in order to protect the intellectual property of the company.

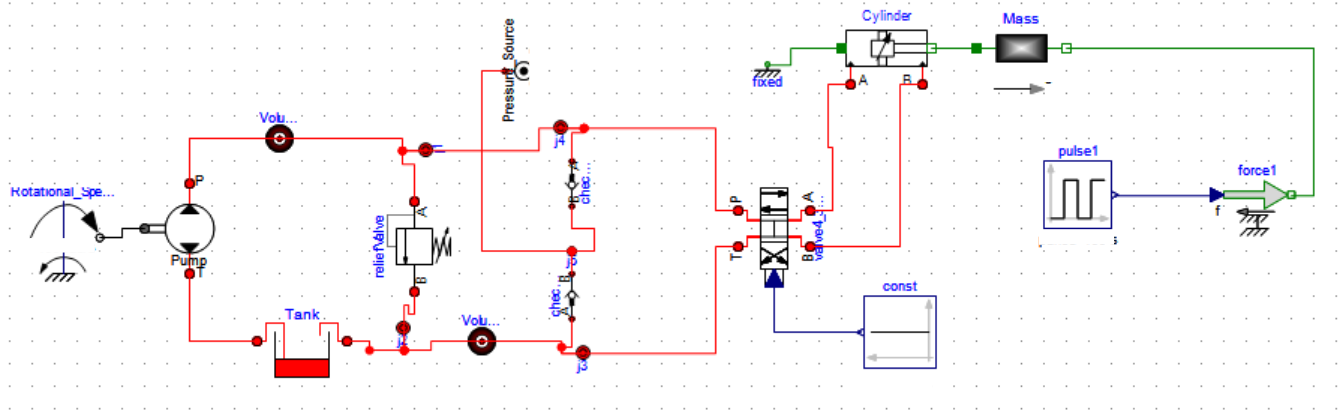


Figure 3.28: EHA model realized with OpenHydraulics

As mentioned previously, the absence of the electric motor is replaced with an element that define a constant rotational speed; this element acts like as input to a *constant-displacement pump*.

A first difference in the models is about the number and type of tanks chosen. In the OpenHydraulics library, the two elements named *simple tank* are considered to infinite volume and do not allow to insert the parameter. Therefore, they have been replaced with a single *Oil Tank* with a double volume respect to the two small reservoirs presented in the SimulationX model. The elements *pressure-relief* valves, connected in both the models with the tanks and the pump, are used to limit the maximum pressure in the system. The relief valve is designed to open at a predetermined set-pressure to protect pressure vessels and other equipment from being subjected to pressures that exceed their design limits. In this case, the valves are used also to return all, or part of the fluid discharged by the pump back to the storage reservoirs. In order to ensure stable operation of the models during the simulation, the elements *volume* have been inserted in the hydraulic connections. Otherwise the valves will try to control the pressure of an infinitely small volume, which is impossible in most situations.

For what concern the *check valve* elements, they are used to model a hydraulic resistance like filters, fittings, bends or armatures depending on the type of flow (laminar or turbulent). Inside the tool, five different flow descriptions are available: two of these are based on the geometry of the flow cross section, while the other three are based on measurement data. The flow description used for the simulation, called alpha-Reynolds description ($\alpha (Re)$), is based on a dimensionless *flow coefficient* α . This coefficient relates the *volume flow* Q to the *pressure loss* Δp according to **Equation 3.13**.

$$Q = \alpha \cdot A \cdot \sqrt{\frac{2}{\rho}} \cdot \sqrt{\Delta p} \quad (3.13)$$

with the *cross section area* A and the *flow density* ρ . The flow coefficient itself is defined as a function of the Reynolds number.

$$Re = \frac{Q \cdot d_h}{A \cdot v} \quad (3.14)$$

with the *hydraulic diameter* d_h and the *kinematic viscosity* v . Reasonable values for α should be in the range of 0,6 – 0,9 considering the flow completely turbulent.

One of the most important element in any hydraulic circuit is the regulation valve that allows to regulate the flow in transit in the actuator. Consequently, it also regulates the force exerted by the actuator and the spool displacement. The chosen element for both the models is a 4/3 proportional-directional control valve, already mentioned in **Section 3.4.2**. This element can be used to model both a servo or a proportional valve. In general, servo-valves have a linear relationship between *spool position* s and *flow area* A , while proportional valves usually have a considerable *overlap* s_0 (generally around 20 %) and a non-linear characteristic between position and flow area.

$$A(s) \sim \begin{cases} (s - s_0)^2 & s \geq s_0 \\ 0 & s < s_0 \end{cases} \quad (3.15)$$

In the models under examination, this valve is practically a switching valve that in steady state is either completely open or completely close. Its command signals are therefore binary signals “on” or “off” (in the models the command signal is defined by a constant function). Inside the element there is a limitation function called *stroking*, that relates the input signal to the stroke signal. The main purpose of this function is to limit the range of the stroke signal: values smaller than -1 are limited to -1, and values greater than 1 are limited to 1, as shown in **Figure 3.29**.

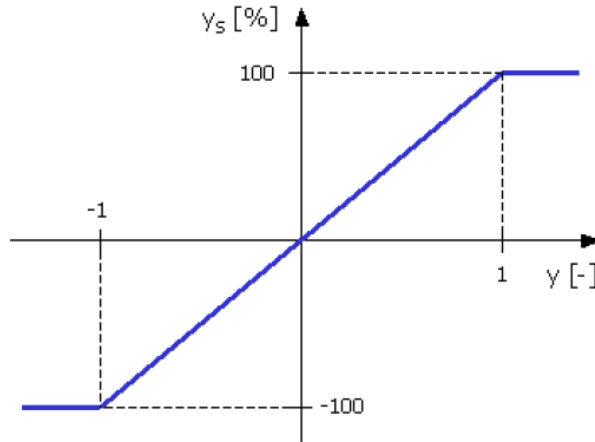


Figure 3.29: Stroke function ^[35]

The fundamental characteristic that must be defined in the valve model is the $Q(y)$ function. This relationship defines the volume flow at certain measurement conditions (in terms of pressure drop, density and kinematic viscosity) that passes through metering orifices. The 4/3 proportional-directional control valve has four different edges¹: *EdgePA* represents the flow restriction between *portP* and *portA*; *EdgePB* represents the flow restriction between *portP* and *portB* and so on. In this case, *EdgePB* and *EdgeAT* are opening edges and *EdgePA* and *EdgeBT* are closing edges, as shown in **Figure 3.30**. The option chosen for the simulation assumes a linear relationship between the relative valve stroke and the volume flow. The user can also specify the lap condition and the flow per stroke ratio for each edge, which in this case are assumed identical.

¹ An *Edge* in this sense is represented by the variable flow restriction between two different ports of the valve. In general, there are two different kinds of edges: opening and closing. An opening edge is characterized by an increase of the flow cross section with increasing stroke signal. In opposite, a closing edge is characterized by a decrease of the flow cross section with increasing stroke signal.

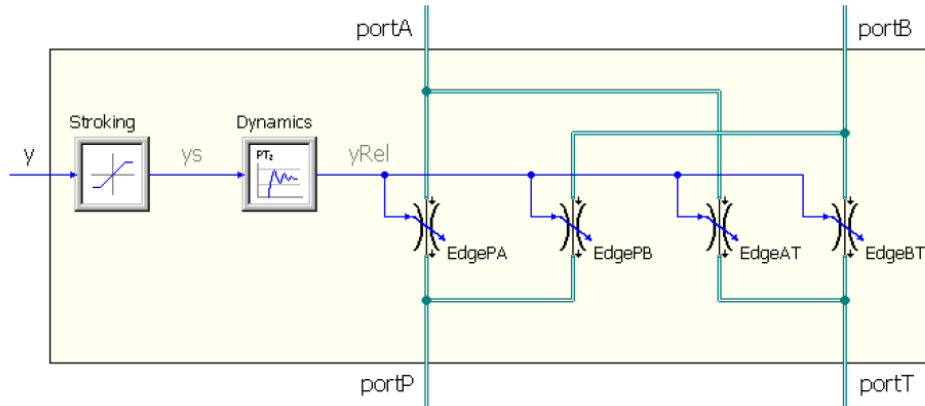


Figure 3.30: Internal view of the 4/3 proportional control valve [\[35\]](#)

The last element that complete the hydraulic circuit is the *cylinder*. Its main function is to convert the hydraulic energy supplied by the pump and by the valves into useful work, or rather mechanical energy.

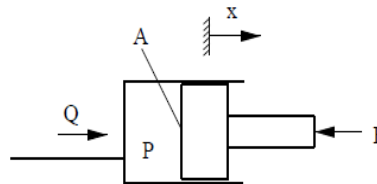


Figure 3.31: Scheme of a single-acting cylinder

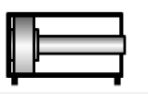
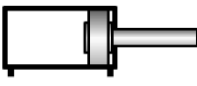
The model of an ideal single-acting cylinder (**Figure 3.31**) is given by simple relations according to **Equation 3.16**.

$$\begin{cases} F = p \cdot A \\ Q = A \cdot \frac{dx}{dt} \end{cases} \quad (3.16)$$

where F is the *actuation force*, p is the *pressure* in cylinder chamber, A is the *piston area*, Q is the *flow rate* and x and dx/dt are the *cylinder position* and the *cylinder velocity* respectively. The chosen element to model the cylinder does not consider any mass inertia. Therefore, the mass inertia of piston must be modelled by connecting the element *mass* to the mechanical connector of the piston. In this case the mass represents also the external load acting on the actuator. In particular, considering an EHA associated with a brake, the external load is represented by the braking force. In the selection window, the user must insert the cylinder

dimensions, the dead volumes and the coordinate transformation between housing and piston dx_h . This parameter defines the displacement difference between the coordinate systems of the mechanical connectors, as presented in **Table 3.4**.

Table 3.4: Typical parameter settings for dx_h ^[35]

dx_h	Cylinder Position	Sketch
0	0	
- maxStroke/2	maxStroke/2	
- maxStroke	maxStroke	

In order to ensure that the piston stroke does not exceed its working range, it is necessary to set up the characteristics of the *end-stop*. The behaviour can be described either as rigid, or elastic. The elastic end-stop model basically works like the *spring-damper*, adding one natural frequency to the system. The velocity difference after the impact is determined by the velocity difference before the impact, by the *end-stop stiffness* c_{stop} , the *end-stop damping* d_{stop} as well as by the mass of the piston. In the rigid end-stop instead the contact with the stops is modelled as an ideal impact, based on the theorem of momentum conservation. When the piston reaches one of the stroke ends, the piston velocity changes immediately within one-time step. The velocity difference in particular is related only with a coefficient k_{stop} . This impact number must be in the range $0 \leq k_{stop} \leq 1$: if $k_{stop} = 0$ the end-stop is considered ideally plastic (inelastic shock), while $k_{stop} = 1$ the end-stop is ideally elastic (elastic shock).

In the simulation, an elastic end-stop has been considered with the adding of a rectangular pulse signal that simulate the braking force. The single signal, with a duration equal to the simulation time, is perceived after 6 s from the beginning of the simulation (*dead-band*). **Figure 3.32** shows the volume flow of the 4/3 control valves in the Edge PB adopted in the two EHA models; **Figure 3.33** shows instead the pressure drop of the two valve models. In both the figures the red line is referred to the responses of the EHA model shown in **Figure 3.28**, while the green line is associated to the responses of the SimulationX model. Despite the trend on the responses is similar, the differences visible in the diagrams are properly linked with the

adoption of two different type of libraries, though the selected elements are the same for both the models. The difficulty therefore in matching the results derived from how the physical behaviour of the elements is modelled, with the use of mathematical equations.

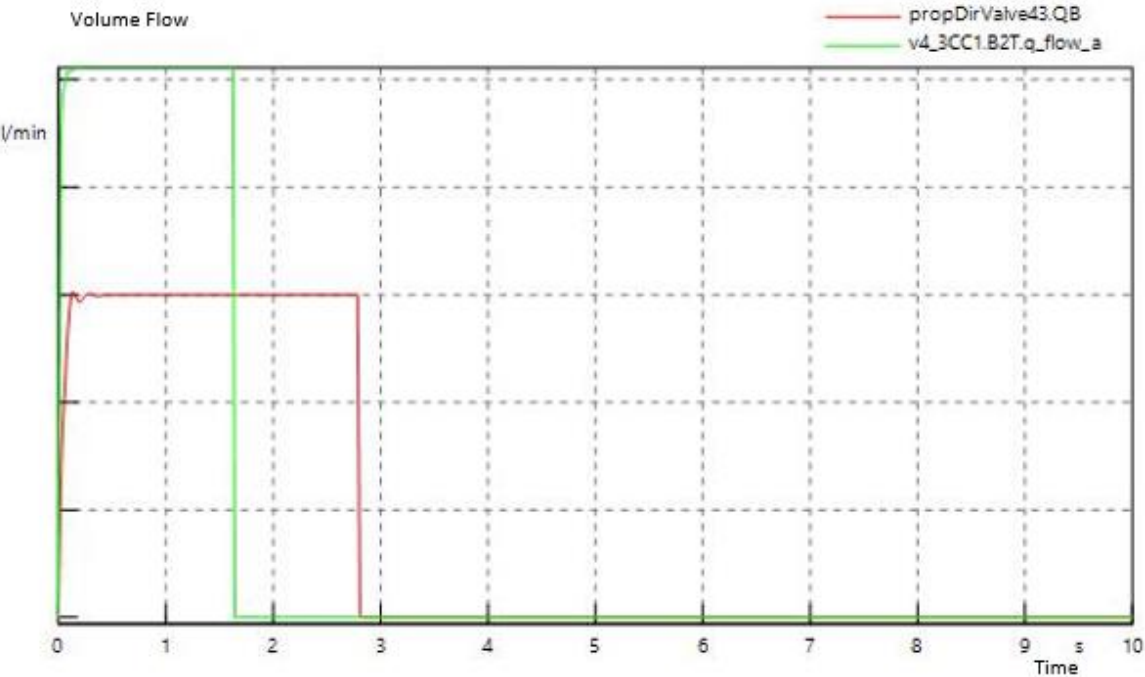


Figure 3.32: Volume flow of the two directional-control valves

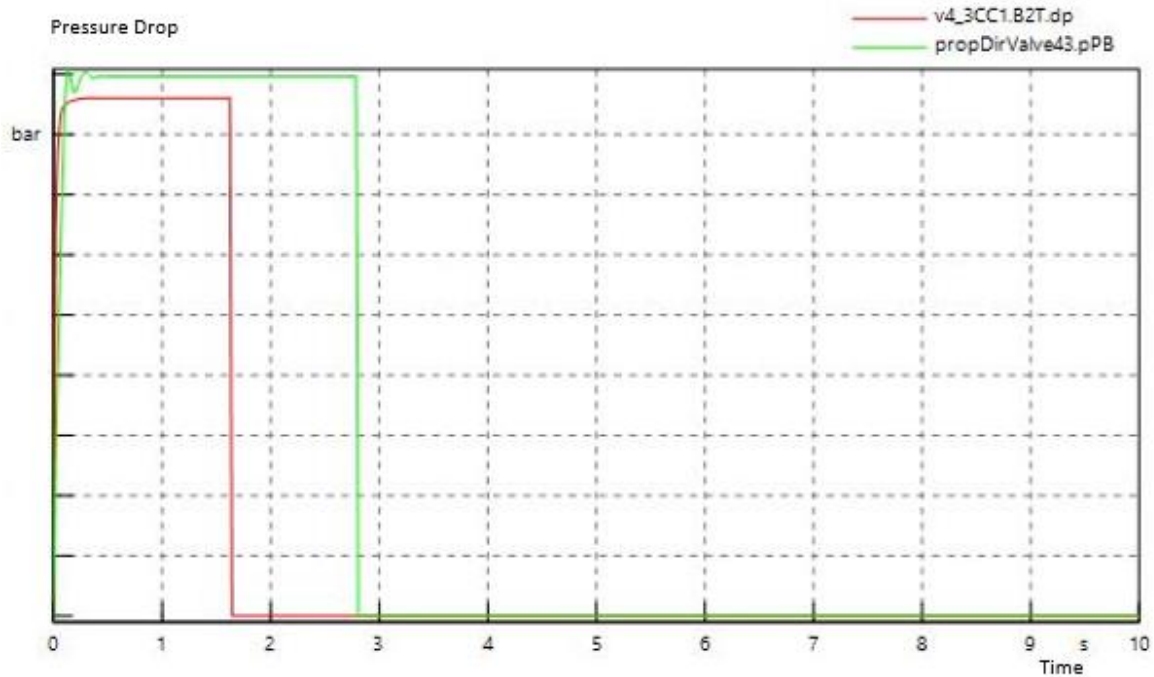


Figure 3.33: Pressure drop of the two directional-control valves

In order to improve the results, *regression tests* have been made. This technique consists in testing every single component of the circuit, starting from the cylinder then from the pump and the valve, varying the same parameters at the same time and comparing the responses. This approach ultimately allows to find the differences in the models deriving from the two libraries. **Figure 3.34** displays simple models realized with OpenHydraulics and SimulationX hydraulic library for doing the regression tests. The models on the left of the figure are developed to test the cylinders, while the models on the right are used to test the 4/3 control valves. Comparing the models, it turned out that the hydraulic parameters such as the maximum pressure in the circuit, the pressure drop in the edges and the nominal flow rate at the nominal pressure cause the greatest differences respect to the geometric and mechanical ones. In this case, the choice therefore of a commercial library is preferred due to its ability to manage the elements and also the parameters in more simple way, without having to recreate additional models or modify their internal equations.

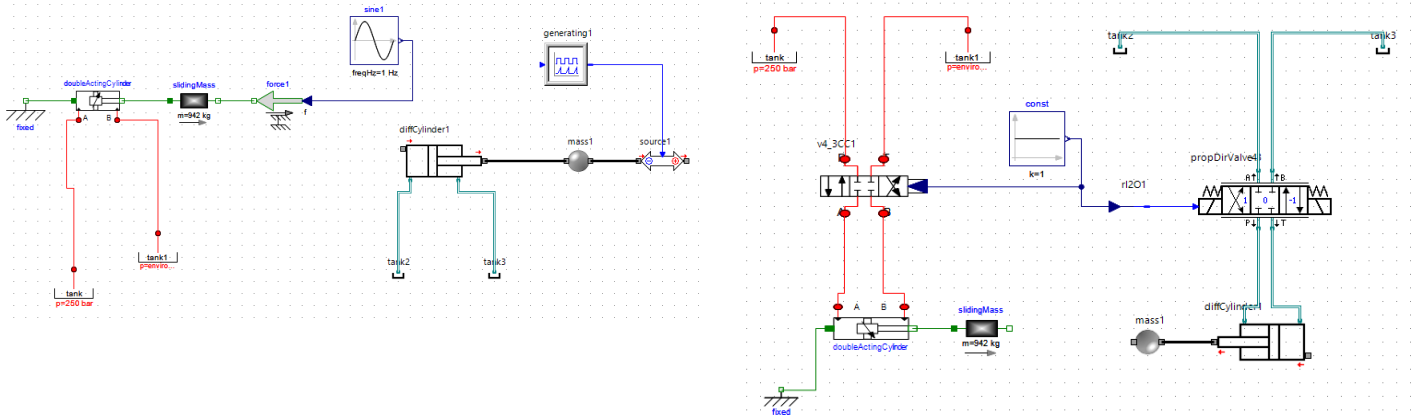


Figure 3.34: Example of regression tests on the cylinder (left) and on the hydraulic valve (right)

3.4.4 Actuator Comparison

In the following section, a description of two different actuator models are presented.

These models, inside the design and optimization chain, can be used: to evaluate the possibility to choose between different feasible architectures with the AEE process, as described in **Section 3.2**; or being integrated into an aircraft model to evaluate the impacts on it and on the other subsystems.

The first actuator model is an EHA, shown in **Figure 3.35**. This model is characterized by a speed command that acts as input for an electric motor that drives a constant displacement pump. The motor used is the same as described in **Section 3.4.3** (with reference to **Figure 3.22**), in which the components are aggregated with the use of the command *compound*. The pressure level and the oil flow are controlled by a 4/3 directional-control valve that feeds the cylinder (both these elements are described in **Section 3.4.3**). The other elements included in the model are:

- The pressure-relief valve, used to limit the maximum pressure in the system;
- The volume, which ensures stability during the simulations (based on what has been already described in **Section 3.4.3**);
- The oil tank.

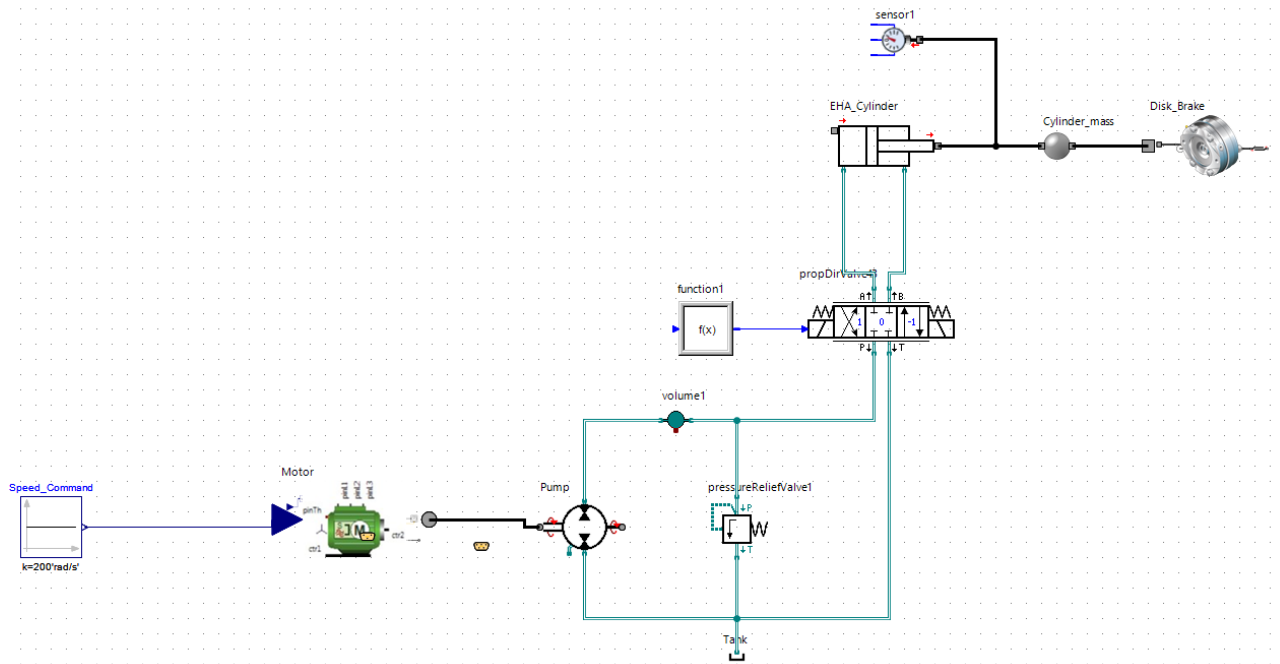


Figure 3.35: EHA model

The second actuator model instead is a SHA, which is illustrated in **Figure 3.36**. In this model all the elements such the motor, the pump and the valves are replaced with a piloted servo-control valve. This valve is a two-stage servo valve, with the 1st stage represented by a 4/3 directional control valve directly linked with the pilot command, while the 2nd stage is characterized by the elements of the custom valve described in **Section 3.4.2**. Also in this case, all the elements of the valve are aggregated with the command compound.

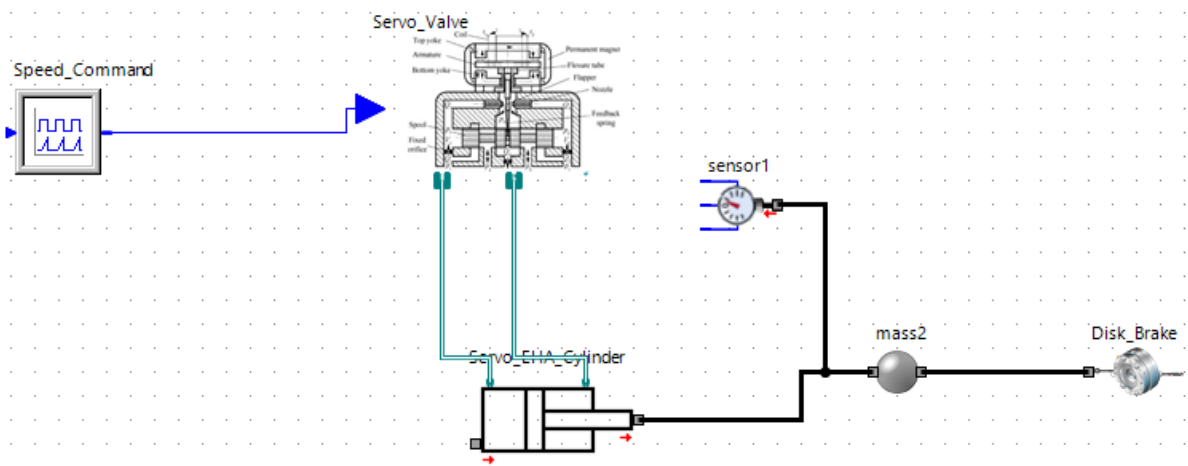


Figure 3.36: SHA model

In both the models, the cylinder is linked with another compound called *Disk_Brake* that represents a simple model of a brake. This compound is well described in the following paragraph.

Brake – Wheel Model

The internal structure of the brake compound is shown in **Figure 3.38**. The first element on the left side of the figure translates rotary force and motion quantities into the corresponding linear quantities and vice versa. In this case, it transfers the *actuation force* (F_{act}) come from the cylinder into the *friction torque* (T_{frict}) according to **Equation 3.17**.

$$T_{frict} = F_{act} \cdot \gamma \quad (3.17)$$

where γ is the *transmission ratio* equal to the product of the wheel radius and the friction coefficient. The *torque* therefore acts as input for the element *Wheel*, which is a physical-oriented model that simulates the contact between the aircraft wheels and the ground. This element estimates a slip value and assigns the friction coefficient according to a prescribed slip

characteristic. In particular, the curve that describes the slip is shown in **Figure 3.37** and it is computed with the definition of four parameters with the reference on **Table 3.5**. This approach is illustrated by Wohnhaas A. et al [\[38\]](#).

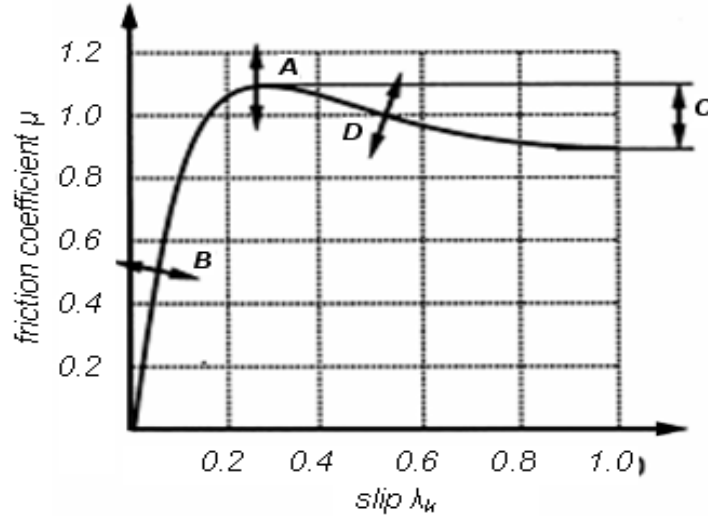


Figure 3.37: Slip characteristic curve [\[38\]](#)

Table 3.5: Values of the four parameters of the slip curve [\[38\]](#)

PARAMETER	INFLUENCE	VALUE
A	Maximum value μ_{\max}	$0.2 < A < 1.2$
B	Slope at origin	$10 < B < 50$
C	Difference to maximum value	$0 < C < A$
D	Turning point	$10 < D < 100$

Once the four parameters are defined, it is possible to calculate the friction with a function illustrated by Wohnhaas.

$$\mu(\lambda_x) = A \cdot (1 - e^{-B \cdot \lambda_x}) - \left(\frac{0.01 \cdot C \cdot e^{D \cdot \lambda_x}}{(C - 0.01) + 0.01 \cdot e^{D \cdot \lambda_x}} - 0.01 \right) \quad (3.18)$$

Normally the *slip ratio* λ_x is evaluated considering the *input-drive speed* v_1 and the *output load speed* v_2 .

$$\lambda_x = \frac{|v_1 - v_2|}{\max(|v_1|, |v_2|)} \quad (3.19)$$

In order to define the friction model applied by the wheel, it is necessary to insert as parameters the *normal force* F_n which acts as load on the wheel and the wheel radius. This value is calculated considering the configuration of the A320, while the force is calculated considering the maximum take-off weight unloaded in the main gear (the normal force is equal to the 70 % of the maximum take-off weight unloaded on the main LG). The selected friction model considers a rigid friction with slipping, but without sticking. The element mass together with the *rigid friction* model shown in **Figure 3.38** represent a simple model of the LG; the mass is equal to the main LG of the A320, while the rigid friction defines the rolling resistance of the wheels.

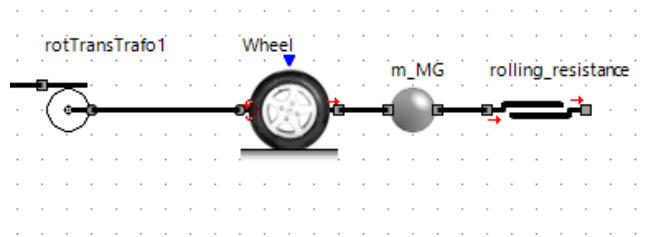


Figure 3.38: Internal structure of the disk brake

In order to compare the EHA model with the SHA, some dynamic simulations have been performed. **Figure 3.39** shows the piston stroke of the cylinder, in which the red line is referred to the SHA response, while the green line is associated to the EHA response. **Figure 3.40** instead displays the rotational speed of the element Wheel. In this figure, the EHA output is represented by the red line, while the green line is the SHA response. The noticeable difference in the rotational speed of the wheel is obviously linked with the different elements involved in the two models. In the realization of the SHA, the topic is focused on the development of the servo-hydraulic mechanism, neglecting therefore some elements. In particular, the pump has been replaced with a simple pressure source, with a maximum pressure equal to the one defined in the EHA fixed-displacement pump. In addition, the adoption of two different valve configurations obviously causes some discrepancies in the dynamic responses. Future detailed analyses, such as the regression tests mentioned above, and a greater fidelity of the models can improve the quality of the results.

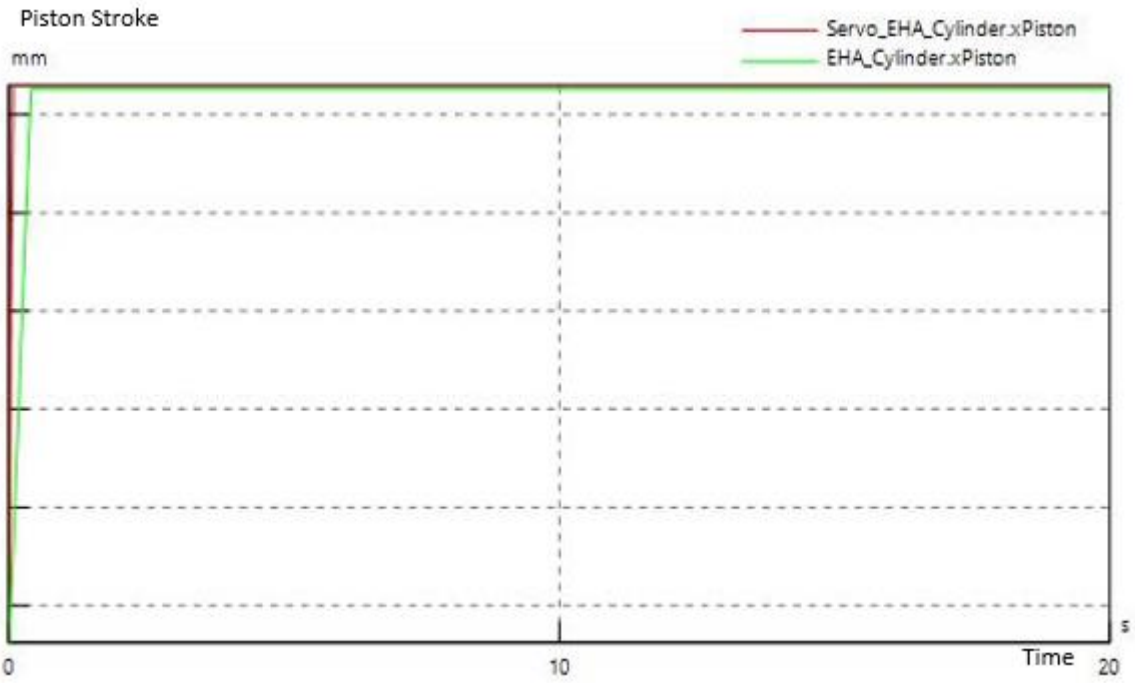


Figure 3.39: Piston stroke of the two actuator models

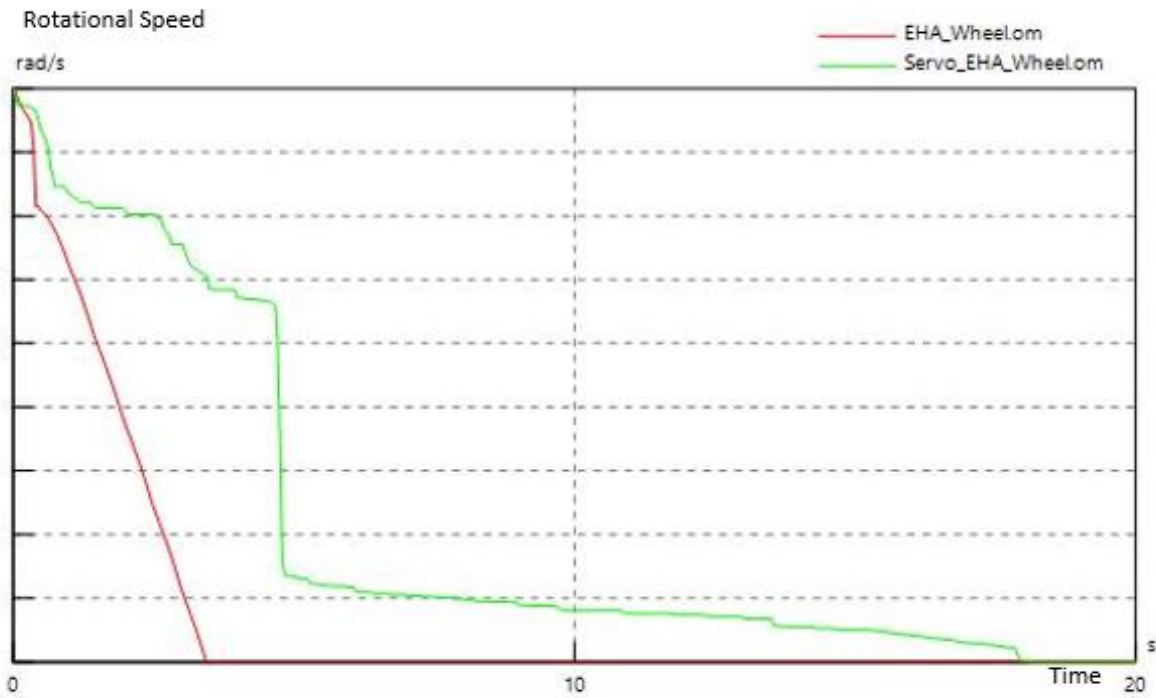


Figure 3.40: Wheel rotational speed of the brake of the two actuator models

3.4.5 Formal Requirement Models

Another key point in the system modelling phase is the formalisation of requirements. This aspect is quite important, since the requirements typically capture the quality of service conditions that a system should fulfil along its lifecycle.

The traditional approach in industrial applications is still to define requirements in textual form, using for example Microsoft Word and managed by tools such as DOORS. Recently, formal approaches to requirements have been developed with the goal to provide representations with a semantic foundation for modelling system requirements. A typical example is the *MODRIO* requirement library [\[39\]](#), which is an open Modelica package to formally define requirements and evaluate them automatically during simulation. Practically, the elements of this library allow to translate a formal requirement into a simulation model that can be associated and run with behavioural models.

This allows first of all to develop an automation process to define formal requirements, causing a considerable saving of time compared to the classic written techniques. In addition, the reusability of these requirement models makes them particularly suitable in the framework of test automation-continuous integration principles and in model-based system engineering approaches. **Figures 3.41** and **3.42** show two formal requirement models associated with the LG, all realized with SimulationX. The first requirement model (defined as *MI-5* requirement number) referred to the *Federal Aviation Regulation* (FAR) 25.109, 25.735 regulations [\[40\]](#) is literally defined as:

“The aircraft shall be able to brake in 600 m (40% of runway) in dry conditions (RTO). Thermal requirements and tyre integrity do not apply in this situation”.

The second requirement (*MI-6* requirement number) taken from the tyre data-book of *Goodyear*, [\[41\]](#) cites:

“The maximum braking force per wheel shall be 50 kN”.

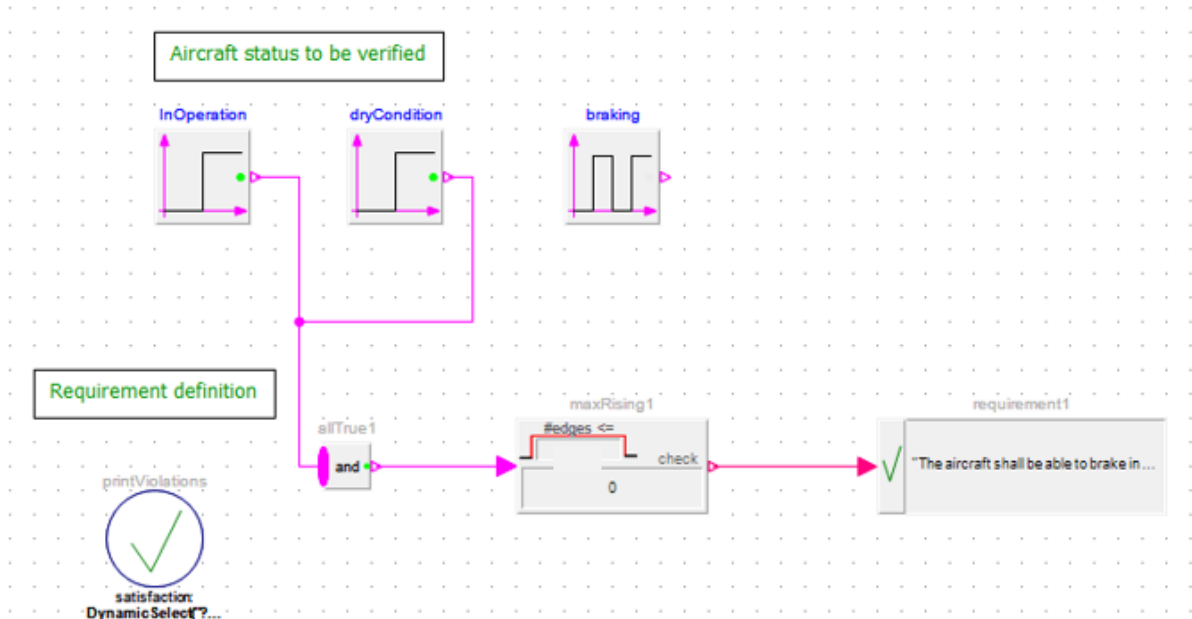


Figure 3.41: MI-5 landing gear requirement model

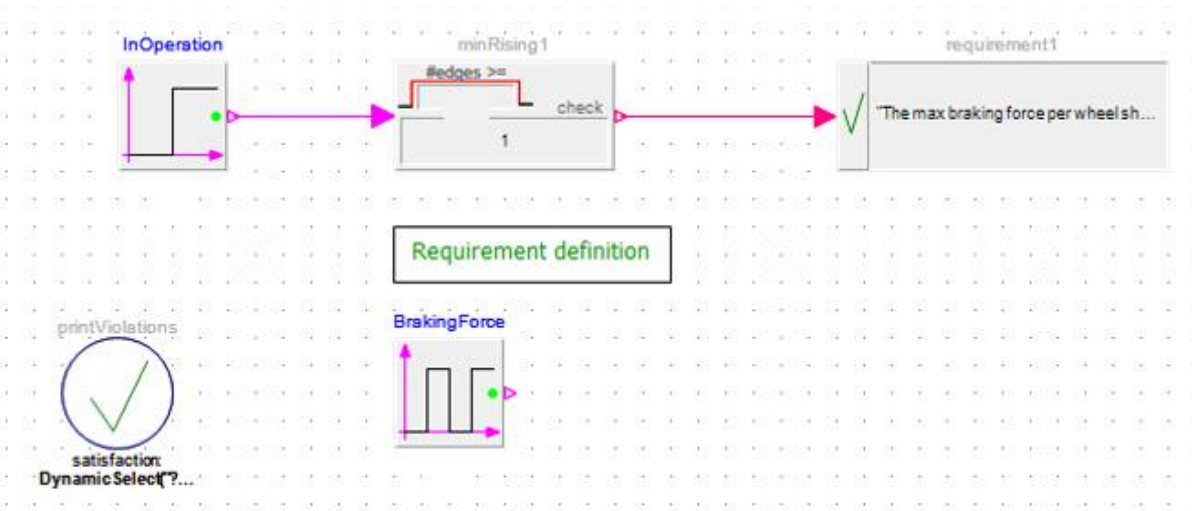


Figure 3.42: MI-6 landing gear requirement model

In both the models, the formal requirement is printed inside an element defined as *Check requirements property*. This model monitors its property input and computes its status at the end of the simulation, which could be:

- Requirement is *Violated*, if the signal input is violated at least once;
- Requirement is *Untested*, if the input is undecided for the complete simulation run;
- Requirement is *Satisfied*, if the input is satisfied at least once, and is never violated.

Another block that is always present in the requirement models is the *Print violated*, which prints a summary of the status of all requirements into a log file in textual format. All the other elements involved are signal blocks of type *Boolean* that are used to “create” the formal requirement model. As outline above, the real importance of develop formal requirements is to combine and test them with physical models, thus speeding up the verification times. **Figure 3.43** shows the MI-6 requirement readjusted for the integration with the EHA model. The first element referred to the requirement takes as input the braking force computed by the Wheel and returns a real expression, which is compared with the parameter *threshold* presents in the second element of the requirement model. This element simply defines the output “*true*” if the input is greater or equal than the threshold, otherwise the output is “*false*”. In this case, the threshold is represented by the max braking force per wheel defined in the requirement.

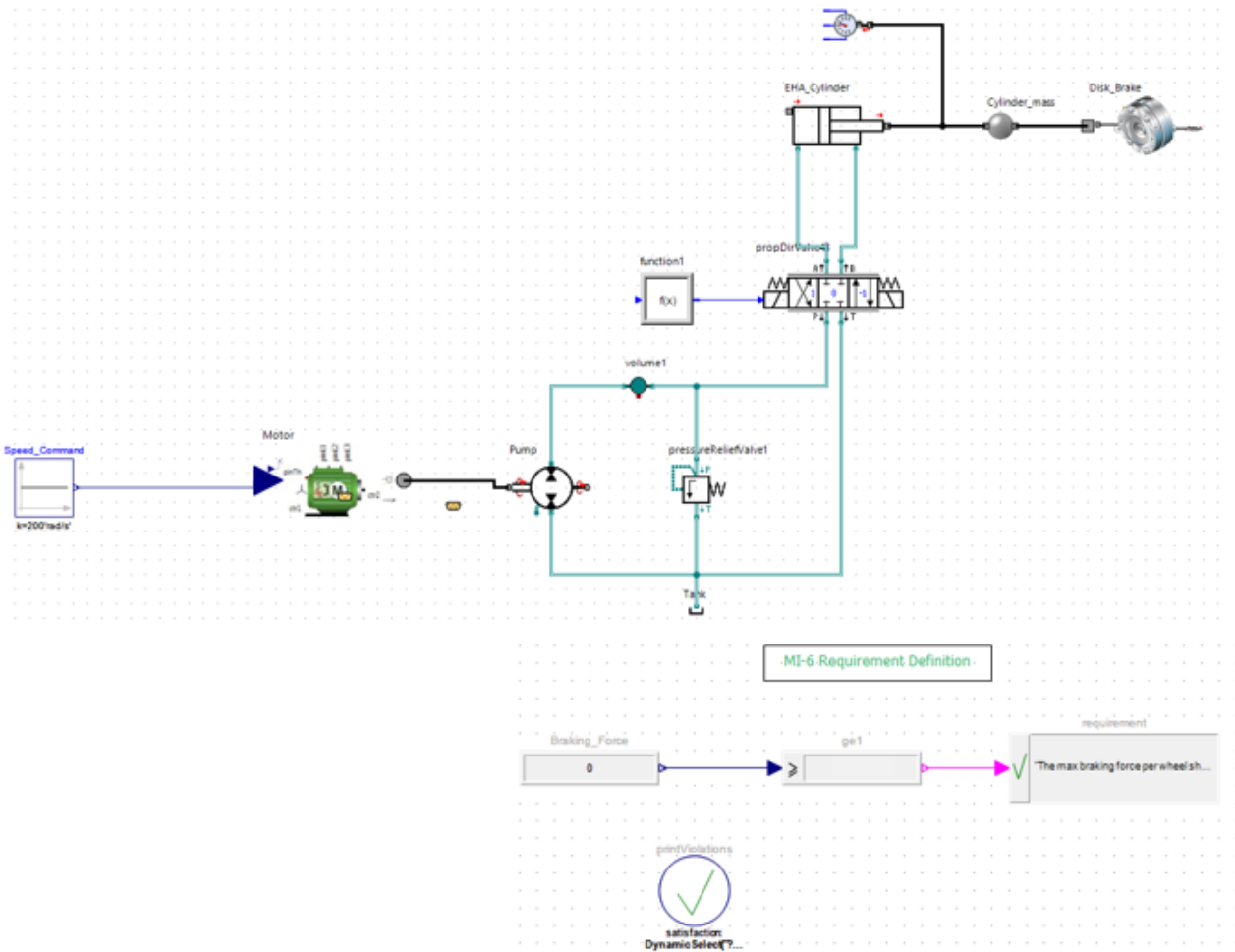


Figure 3.43: EHA model with the MI-6 landing gear requirement model

Running the simulation, the result printed in the text file shows that the requirement is violated. This because the braking force, that is shown in **Figure 3.44**, remains constant until 6 s, then decreases to 0 with some oscillations when the wheel is totally braked. Therefore, the requirement remains satisfied until the force change its value like shown in **Figure 3.45**, that represents in percentage the satisfaction of the requirement during the simulation time.

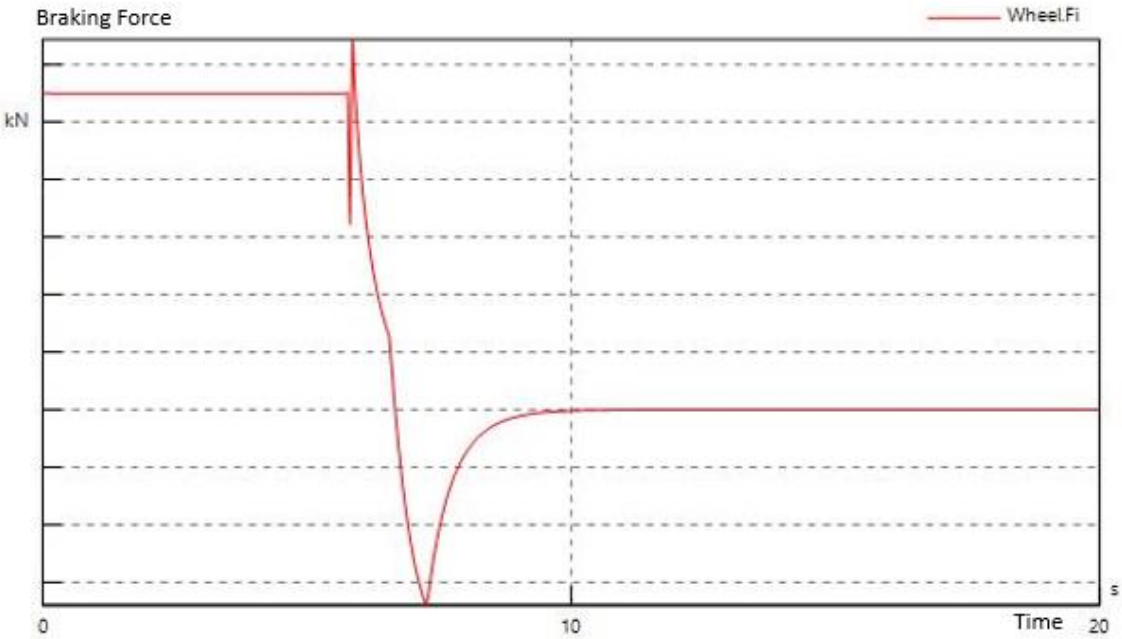


Figure 3.44: Braking force on the wheel

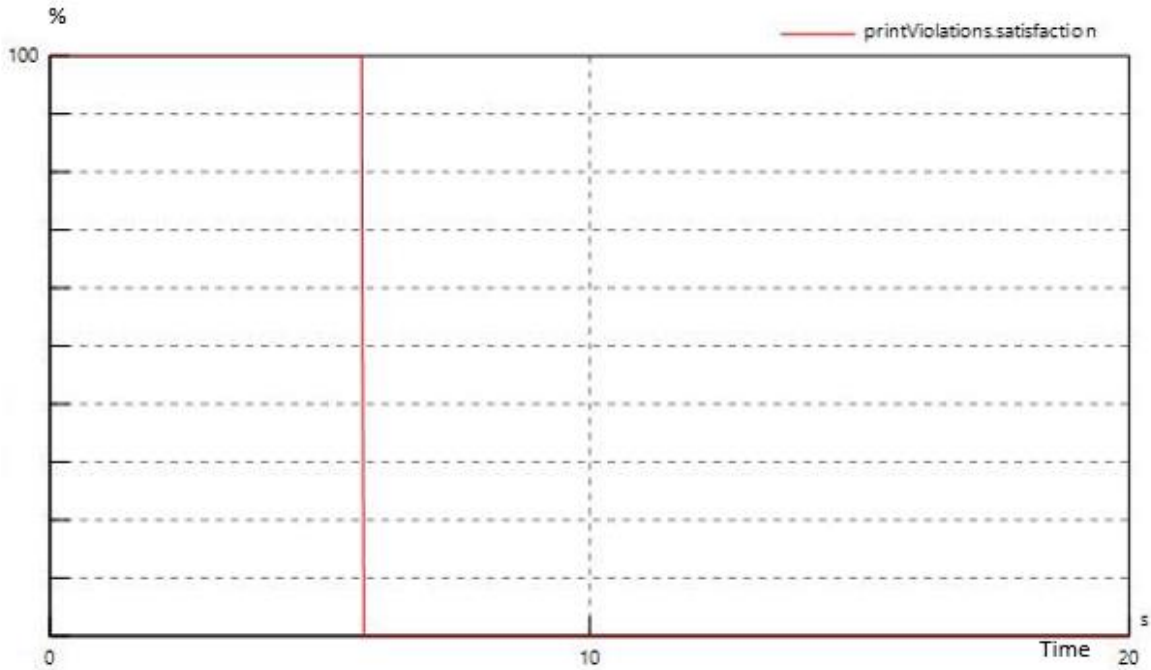


Figure 3.45: Requirement satisfaction in percentage

This modelling activity is shown for purpose of illustration and not all the requirements captured are translated as models. Inside MISSION, there is an activity planned in one work package on formalising requirements and building an augmented test model (models + test scenario) to evaluate such formal requirements.

4. DESIGN OPTIMIZATION

4.1 Generic Optimization Workflow

As already mentioned in the previous sections, one of the main goal of MISSION – and more in general of Clean Sky 2 projects – is to develop new technologies to make aircraft more competitive, greener and safer. In this sense, the use of electric technologies such as EHA in more-electric aircraft may potentially reduce significantly aircraft weight and maintenance costs eliminating the centralized hydraulic system. For example, A380 saves over 450 kg introducing two redundancy power-by-wire actuation systems in the FCS [\[42\]](#). Applications of EHA's to aircraft brake are only at early stages of conception and approaches that are described in this work may help in such studies. Therefore, it is important and interesting to optimize the actuator performances in the preliminary design phase and then evaluate their impact at aircraft level. In particular, for an EHA, the key performances can include light-weight, high efficiency, quick dynamic response and low cost.

The design optimization activities carried out in this work are not focused on optimisation techniques (for example answering is it optimal in a mathematical sense or which is best approach to do this optimisation), but rather building the component models which can be used both in architecture definition, design optimisation and integration. The goal is therefore to couple performance models, in particular the sizing model realized with the MATLAB scripts (presented in **Section 3.3**) with the physics-oriented ones developed with SimulationX (the various actuator models presented in **Section 3.4**), to get the best possible design or to explore design space adequately respecting some performance and non-performance criteria, such as the mass, the efficiency, the cost and so on. Though the optimization approach described may appear relatively simple, in reality this involves many stakeholders, multiple iterations and additional analyses between them. From this point of view, it becomes difficult to associate the performance models, since they are usually done by separate people, namely system modeller (or designer) and preliminary system designer. In addition, these models are exploited for optimization by an expert in optimization techniques, who usually does not have system design knowledge, but rather focused on numerical aspects of optimization [\[15\]](#).

In order to have a clearer view how this optimization workflow is carried out, a logical scheme is presented in **Figure 4.1**. As first step, all the three persons involved namely, designer, modeller and optimization expert should be agreed on a typically architecture definition to develop individual components, defining the optimization problem. Subsequently, the designer starts to develop for example MATLAB scripts or excel sheets to give a first estimate of components parameters. Similarly, the modeller with the use of simulation tools creates dynamic models, which are tested and run with the use of the design parameters estimated by

the designer. Since the two models are realized in two different environments, not all the estimate parameters can be associated between the two models. For this reason, a template called *design dependency matrix* must be filled together by designer and model developer to clearly understand the dependency between the models. Finally, the optimization expert chooses the solver, tool and techniques to generate reduced order models and then performs a *multi-objective optimization* analysis (MOO) getting the data from both the performance models.

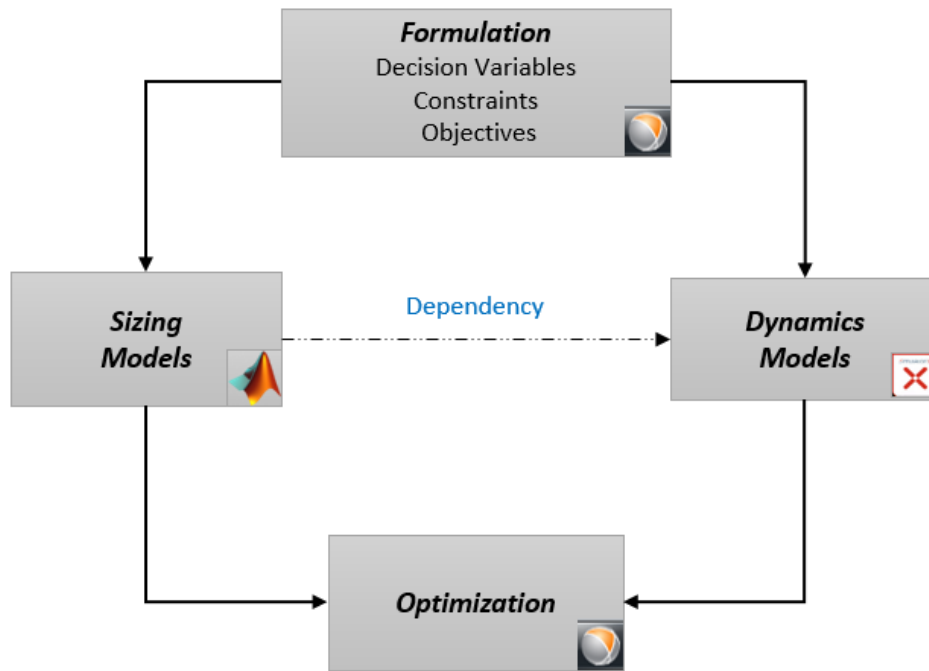


Figure 4.1: Optimization workflow

4.2 Multi-Objective Optimization Problem

A typical MOO problem can be defined by the subsequent formulations [\[43\]](#).

$$\begin{aligned}
 & \text{Minimize/Maximize} && f_m(x) && m = 1, 2, \dots, M \\
 & \text{Subjected to} && g_j(x) \geq 0 && j = 1, 2, \dots, J \\
 & && h_k(x) = 0 && k = 1, 2, \dots, K \\
 & && x_i^{(L)} \leq x_i \leq x_i^{(U)} && i = 1, 2, \dots, n
 \end{aligned} \tag{3.20}$$

with $x = (x_1, x_2, \dots, x_n)$ is the vector of the *design variables*, which are all the system parameters ranging from a lower L to an upper U limit to find the optimal design. $g_j(x)$ and $h_k(x)$ represent instead respectively the *constraints of inequality* and *equality*. The solutions are all which comply with both constraints and variable bounds. In particular, each solution x is assigned to a vector $f_x = z = (z_1, z_2, \dots, z_n)$ describing one point of the M-dimensional objective space.

Several procedures have been developed to solve a MOO problem. One of the most common consists to transfer the multi-objective problem into a single-objective one in two ways: choosing a preferred objective function and introducing the remaining objectives as constraints; or combining all objectives in a single function using individual weights.

Figure 4.2 shows the flowchart of the MOO procedure. After defining the design variables, the various inputs and constraints, a *sensitivity analysis* may be done before optimisation, in order to assess the impact of the design variables on the objective function. By definition, a sensitivity analysis is: “*the study of how the uncertainty in the output of a model can be apportioned, qualitatively or quantitatively, to different sources of variation in the input of a model*” [\[44\]](#) (Saltelli et al. 2008). This study is done to analyse the impact (the sensitivity) of the design variables variation with respect to the results and also which of the design variables have not appreciable impact on the outcome of simulation. In this way, it is possible before starting the optimization to discard the design variables not useful for the analysis.

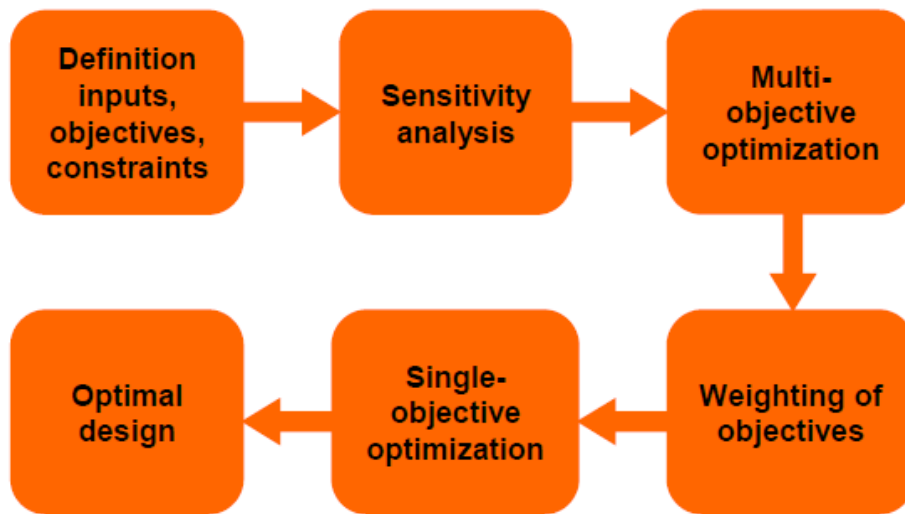


Figure 4.2: Multi-objective optimization logical flowchart ^[43]

4.3 Optimization Implementation

4.3.1 Choice of Design Variables and Constraints

The optimization approach where the performance models are integrated to perform the analysis is made with the use of a tool called *OptiSLang* ^[45]. The method illustrated in this thesis is applied to demonstrate the resolution of a typical optimization problem. In particular, the described problem is single-objective, because it has been considered only one objective function.

Following the workflow presented in **Figure 4.1**, the first step consists to define the inputs of the analysis or rather the design variables and the constraints, according to the system requirements. In the specific case, the key design drivers of an EHA can be chosen analysing the brake formal requirements. The first design variable is the *piston stroke*. This parameter, being an input of the sizing model explained in **Section 3.3**, it influences all the geometric aspects of the cylinder and therefore its configuration and then the maximum actuation force that it is able to generate. The second variable is about the pump, in particular the *pump speed*. This parameter, with the pump displacement, delineates the size of the pump and impacts also in the electric motor performances (motor torque and speed). The last design variable is the *transmission coefficient* K_p between the pump torque and the motor one. This parameter considers the possible mechanical losses and the friction in the transmission between the two elements.

The constraint chosen for the optimization analysis is associated with the *maximum motor power*. Since it is proportional both to the motor torque and speed, reducing its value means limit both. In particular, the motor speed must be maintained under certain values to avoid mechanical problems on the transmission shaft and losses. Also, the torque, being associated with the motor saturation current, cannot be too high, in order to avoid Joule losses in the motor armature.

With the reference of **Table 4.1**, the ranges of the design variables and the constraint related to the electric motor power are shown. These values are chosen analysing literature cases [31][46] and system catalogues [47][48]. In order to protect the data produced internally in UTRC-I and to respect the ITC policy of the company, the tables above show no-numerical values.

Table 4.1: Design variables and constraint of the optimization problem

DESIGN VARIABLE	VALUE	UNIT	CONSTRAINT	VALUE	UNIT
STROKE	$\text{strk}_1 \leq \text{stroke} \leq \text{strk}_2$	mm	MOTOR POWER	$P_m \leq (P_m)_{\max}$	W
PUMP SPEED	$\omega_{p1} \leq \omega_p \leq \omega_{p2}$	rpm			
TRANSMISSION COEFFICIENT	$K_{p1} \leq K_p \leq K_{p2}$	/			

4.3.2 Optimization Objective and Case Study

Weight is one of the most crucial aspect in any aerospace system design. Therefore, the objective function of the optimization is focused to minimize the mass of a single EHA, obtaining therefore possible weight reduction of the entire brake system and other benefits at A/C level such as fuel burn, reduction of power consumption and so on.

The optimisation at aircraft level has not been presented in this work, due to the lack of a detail A/C model. Besides, its integration with the other two performance models would be complex considering all the variables involved. Some preliminary results at A/C level are therefore evaluated in the MISSION framework, thanks to the collaboration between UTRC and the partners.

In this study, the optimization is evaluated for two different cases in order to evaluate and compare different results:

- *Study Case 1*: the sizing model is the one described in **Section 3.3.1** which is associated to the EHA with the servo-motor model (with the reference on **Figure 3.23**).
- *Study Case 2*: the sizing model is the one combined with the similarity-law method (described in **Section 3.3.2**) associated to the EHA with the electric motor model developed with the A-2015 library (with the reference on **Figure 3.22**).

Once the dependency between the performance models has been clearly defined, or rather which are the parameters that are passed and varied at every simulation run, OptiSLang creates a “template” with the connection between the models. This template, shown in **Figure 4.3**, is a kind of black box similar to the partial model described previously, which are filled with the models illustrated in the two study cases.

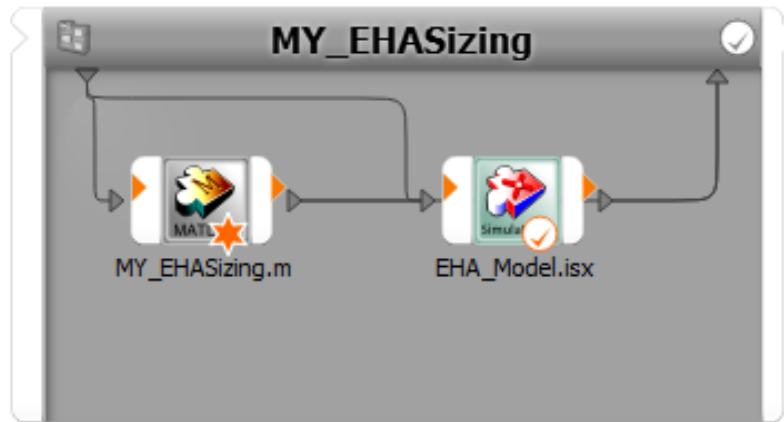


Figure 4.3: General template of OptiSLang

At this point, it is possible to start the sensitivity analysis dragging and dropping in the template a specific item called *sensitivity wizard*. Depending on the design variables involved and their ranges, the tool suggests the best method to perform the analysis. In particular, in both the cases described a method based on *Latin Hypercube* is applied [43]. This mathematical approach is a stochastic sampling method widely used in *Monte Carlo* simulation, to generate random samples of parameter values. By definition, a *Latin Square* [49] is a square grid containing sample positions, where there is only one sample in each row and each column. A *Latin Hypercube* is the generalisation of this concept to an arbitrary number of dimensions, whereby each sample is the only one in each axis-aligned hyperplane containing it. Given a function of N variables, the range of each variable is divided into M equally probable intervals; M sample points are then placed to satisfy the *Latin Hypercube* requirements. For more detail about the method, the reader can refer to Iman, R. and Conover W. [50].

In the same way done for the sensitivity analysis, the optimization is exploited dragging and dropping the *optimization wizard*. In this case, the applying method for the two study cases is called *Adaptive Response Surface Method* [43]. This approach is part of the *Design of Experiments* (DoE) methods [51] used to approximate an unknown polynomial function for which only a few values are computed. The procedure starts with the realization of a single DoE scheme as the initial centre point. Based on the approximation of the model responses, the optimal design is searched within the parameter bounds of the DoE scheme. After the first

iteration step, a new DoE scheme is built around this optimal design. The scheme is moved, shrunken or expanded, depending on the distance between the optimal designs of the current and previous iteration steps. The algorithm converges if the change of the optimal design position and its objective value between two iteration steps is below a specified tolerance; or if the DoE is shrunken to a minimum size. More details about the procedure can be found in Etman L. et al [52].

Finished the whole simulation, OptiSLang creates the complete optimization template that is shown in **Figure 4.4** (the template is the same for both the study cases).

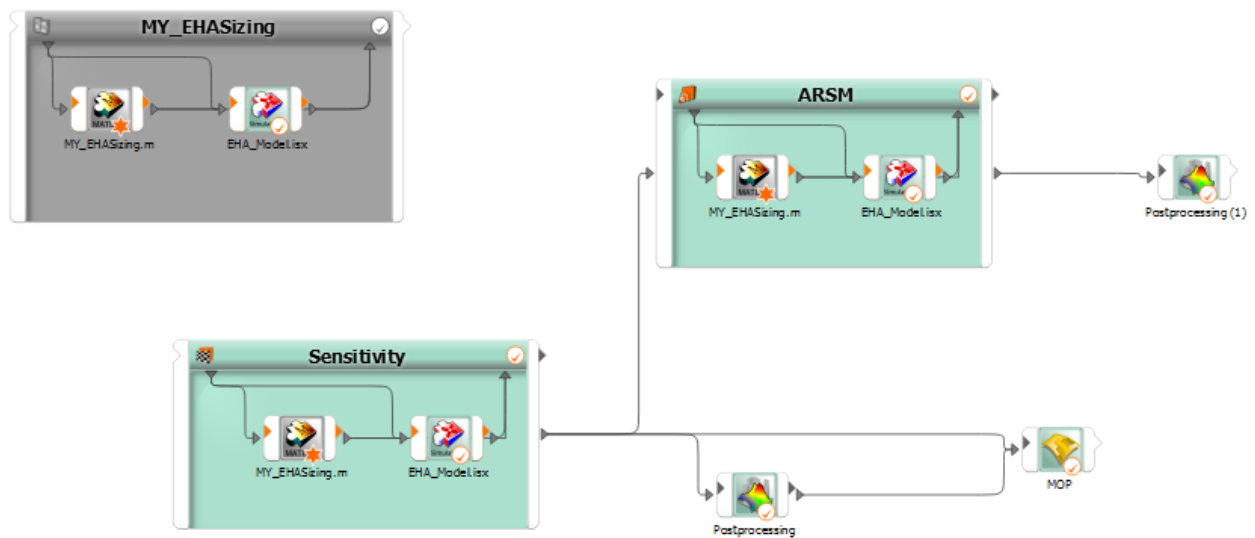


Figure 4.4: Complete optimization implementation template

In the next paragraphs, the results of the sensitivity and the optimization analysis are presented for both the study cases.

Study Case 1

One of the relevant outcome of the sensitivity analysis is the correlation matrix that defines the correlation between the design variables, the objective function and the constraint. This dependency is evaluated with coefficients called *Coefficients of Importance* (CoI), that quantify the input variable importance using the *Coefficient of Determination* (CoD) measure [43]. Based on a polynomial function, the CoI of a single variable X_i with respect to the response Y is defined according to **Equation 3.20**.

$$CoI(X_i, Y) = CoI_{Y, X_i} = R_{Y, X}^2 - R_{Y, X \sim i}^2 \quad (3.20)$$

where $R_{Y, X}^2$ is the CoD of the full model and $R_{Y, X \sim i}^2$ is the CoD of the reduced model, where all terms belonging to X_i are removed from the polynomial basis. These coefficients represent the relative amount of variation explained by the approximation given by Montgomery D. and Runger G [53].

The following diagrams show the CoI's expressed in percentage in order to quantify the design variables importance. In particular, **Figure 4.5** shows the CoI's of the three design variables chosen in relation to the objective function of the problem (the minimization of the EHA mass). **Figure 4.6** instead displays the CoI's in relation to the constraint (the electric motor power). From both the diagrams it is possible to notice how the *transmission coefficient* K_p is the design variable that affects more both the outputs, despite the CoI associated to the pump speed is lightly high in the outcome related to the constraint.

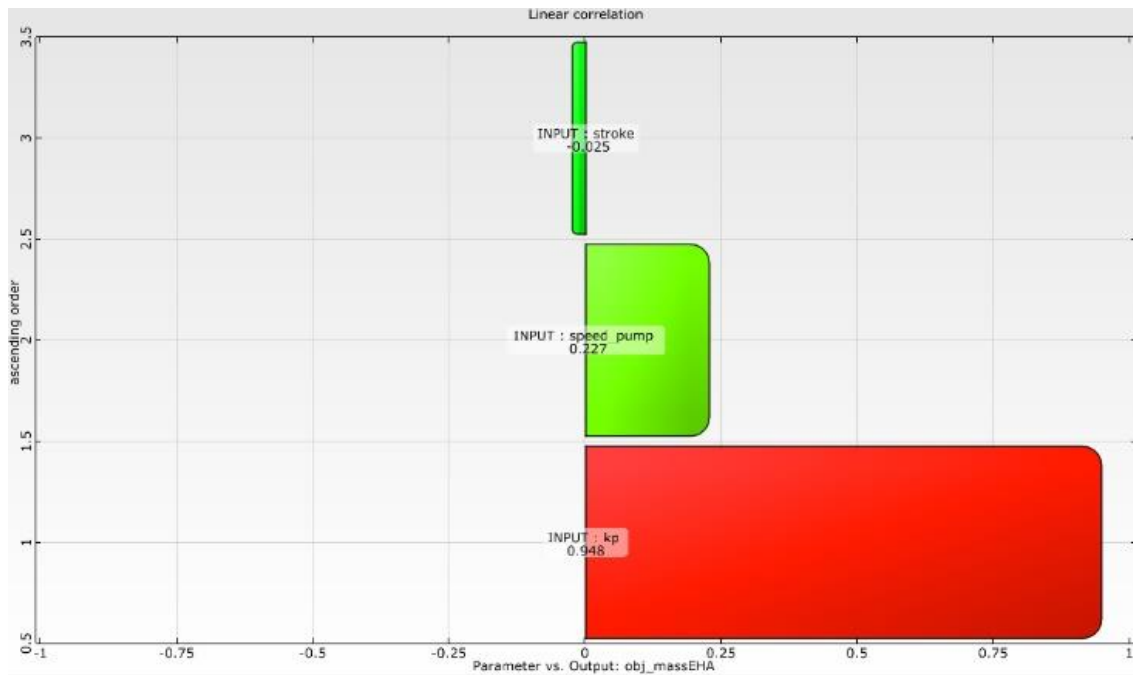


Figure 4.5: *CoI as a function of the objective function (Study Case 1)*

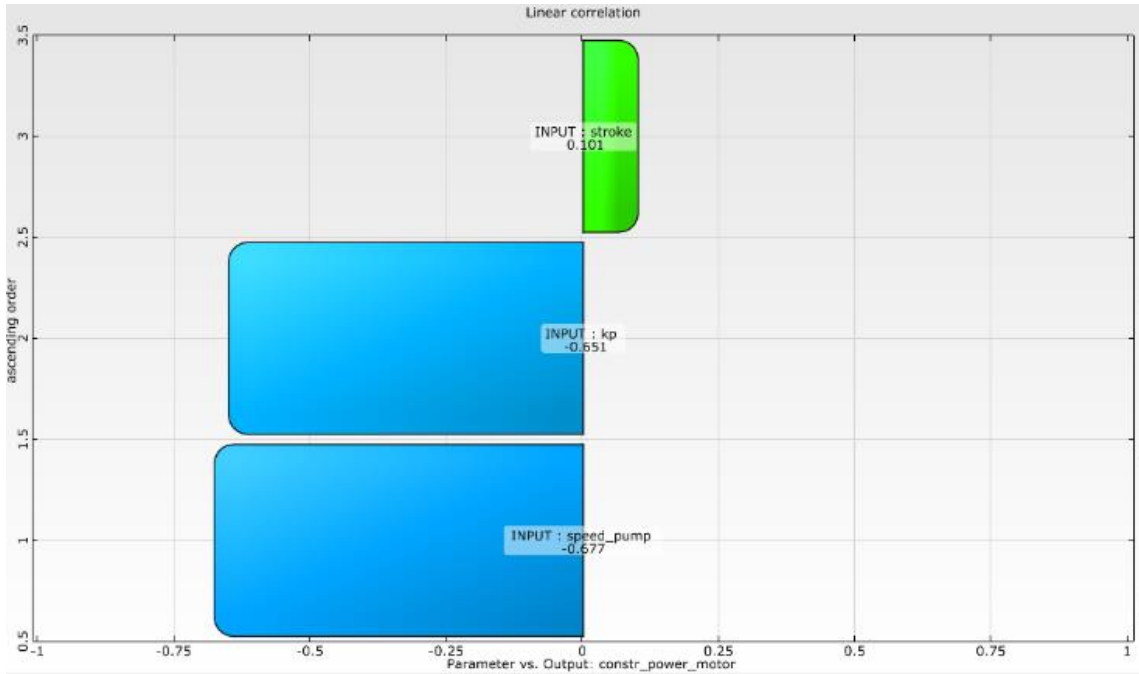


Figure 4.6: *CoI as a function of the constraint (Study Case 1)*

For what concern the optimization results, they are presented in **Table 4.2** starting from the outputs of the sensitivity analysis. The optimal design point shows how the EHA mass is decreased significantly combined with the values of the decision variables. The values K_{p1} , ω_{p1} and $strk_1$ presented in the table are referred to the lower limit of the variation range of the design variables (with the reference of **Table 4.1**). These results from a system point of view can be considered acceptable, comparing the typical values associated to an EHA findable in literature [46]. However, the results are not yet validated and is being done with the corresponding business units in future. It must be stressed that the objective is to build candidate models and tools to perform such design optimisation tasks and not the validation per se.

Table 4.2: *Optimization results of the Study Case 1*



Study Case 2

Also for this study case, the diagrams referred to the CoI's are presented: **Figure 4.7** shows the relation between the CoI's and the objective function; **Figure 4.8** displays the CoI's in relation to the constraint. The sensitivity analysis outcomes show again that K_p is the dominant variable on the responses. The only difference is associated with the CoI of the pump speed that results minor on the output response of the objective function, then the value shown on the **Study Case 1**.

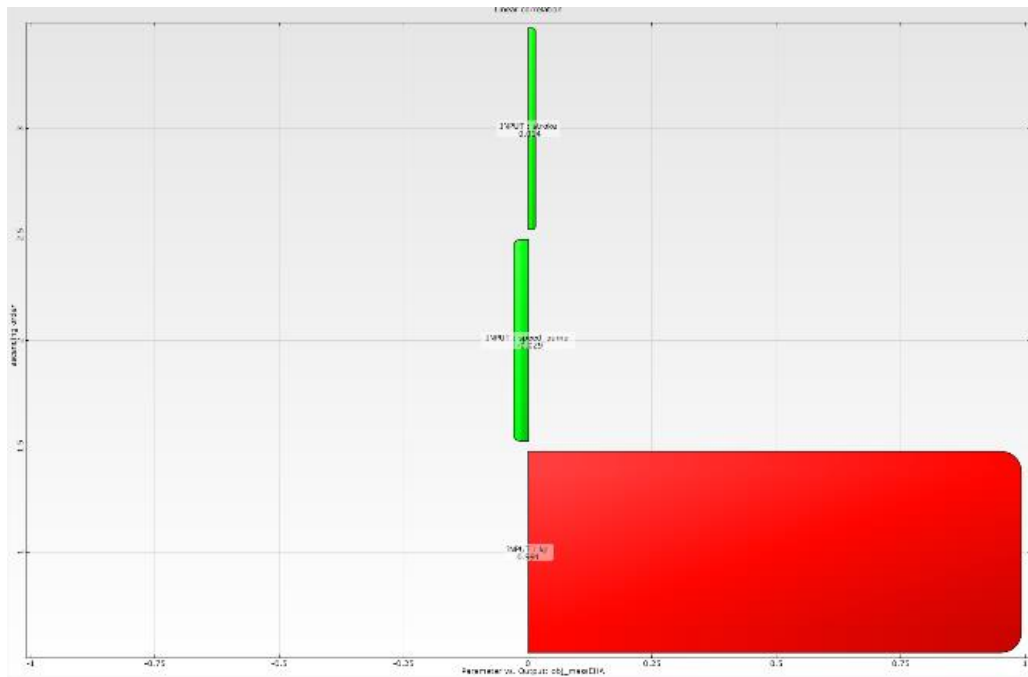


Figure 4.7: CoI as a function of the objective function (Study Case 2)

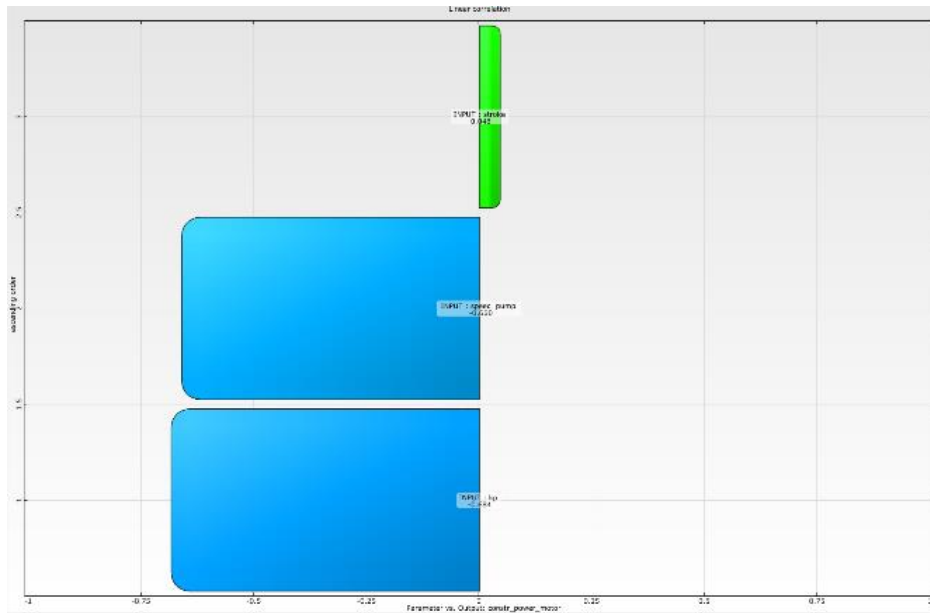
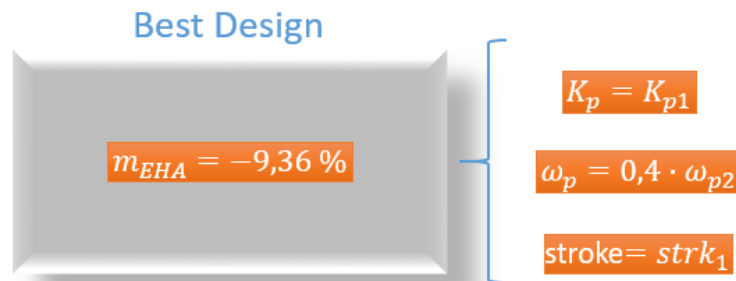


Figure 4.8: CoI as a function of the constraint (Study Case 2)

Table 4.3, referred to the optimal design point of this study case, shows differences on the optimization results compared to the previous optimization analysis. The similarity laws adopted to size the motor cause an initial increase on the EHA mass, as shown in Table 3.3. Nevertheless, the optimal design point presented in Table 4.3 shows that the mass is decreased less than in the Study Case 1. For what concern the design variables, the optimization analysis indicates that the stroke and the transmission coefficient are optimized on the same values for both the cases, while the pump speed is increased around 40 % (respect to the upper limit). This because the pump is characterized by a greater displacement and a greater speed, being powered by an electric motor that results lightly oversized using the similarity laws.

Table 4.3: Optimization results of the Study Case 2



Although this optimization approach is limited only on mass and performances, it could be well extended to other domains such as thermal analysis, manufacturing, cost, reliability and so on.

5. CONCLUSIONS AND FUTURE WORK

This thesis proposed a multidisciplinary framework for landing gear brake actuation design as part of landing system design and integration activities in the MISSION project. Sizing and physic-based models of electro-hydrostatic actuator and servo-hydraulic actuator for the aircraft brake systems have been developed, in order to analyze a sizing, evaluation and optimization workflow carried out in MISSION. Once the estimation models have been developed and obtained the sizing parameters of the actuator components, several modeling and simulation activities has been performed to evaluate the possible uses of these new actuation devices in new generation aircraft. A design optimization analysis has also been executed to analyze some actuator performances.

The results presented with this work demonstrated that the model library is suitable for exploration and evaluation purposes, in support of the design of novel improved actuation solutions. In particular, this work is partially done with some preliminary results that are presented in some deliverables of MISSION project.

In addition, these models can also be integrated at aircraft level to emulate the typical interaction between airframers (who build the aircraft model) and system suppliers (who build the system model) in the design process. In this way, it is possible to evaluate the effects of the integrated systems on different A/C metrics such as the power consumption, the fuel burn, the number of missions. For more details on this study, the reader can refer to the public available work presented by Cimmino N. et al [\[54\]](#).

It has been analyzed how the use of sizing models can support the preliminary design process, when high fidelity parameters are not available. It has also been shown how the use of an a-causal modeling language (Modelica) and the development of reusable component libraries and partial models are particularly helpful for physics-based modeling activities. Moreover, thanks to the adoption of open interfaces, it is possible to easily exchange models between different tools with the use of FMI standards.

In addition, it has been demonstrated that the optimization analysis gives the optimal design point associated to the EHA mass. Based on the chosen design variables, an effective reduction in the weight of the actuator has been obtained.

Potential areas for future research related to this work could include:

- The application of multi-objective optimization problems with the prediction of cost, efficiency and other dynamic performances of the EHA.
- The improvement of the fidelity of the models considering, for example, thermal and electrical losses. In this way, these models could feed the various aircraft platforms, especially improving the analysis related to the power platform [\[24\]](#) [\[26\]](#) and the thermal one.
- The development of control design systems applicable to the realized models to increase the quality of the dynamic results in the simulations.

REFERENCES

- [1] International Air Transport Association; 2016; “Air passenger forecast: Global Report”; Montreal, Canada.
- [2] Blyler J. “THE SYSTEM LIFE CYCLE”. Website: <http://jbsystech.com/system-life-cycle/>.
- [3] V. Valdivia-Guerrero, R. Foley, S. Rivero, P. Govindaraju, A. Elsheikh, L. Mangeruca, G. Burgio, A. Ferrari, M. Gottschall, T. Blochwitz, S. Bloch, D. Taylor, D. Hayes-McCoy, and A. Himmler. “Modelling and simulation tools for systems integration on aircraft”. In *SAE Technical Paper*. SAE International, 09 2016.
- [4] Torsten Blochwitz (ITI), Martin Otter (DLR-RM). “The Functional Mockup Interface for Tool independent Exchange of Simulation Models”. In *Modelisar 2011*, 21st, 22nd March.
- [5] AUTOSA; “AUTomotive Open System Architecture”, 2017. Website: <http://www.autosar.org>.
- [6] ARINC; “Standards Development Document”, 2017. Website: <http://www.aecamcfsemc.com/standards>.
- [7] Y. P. Guo, K. J. Yamamoto, R. W. Stoker. “Component-based empirical model for high-lift system noise prediction”. *Journal of Aircraft*, 40(5):914, 2003.
- [8] B. Allison, M. Roth, I. Kokkolaras, P. Kroo Papalambros. “Aircraft family design using decomposition-based methods”. In *11th AIAA/ISSMO Multi-disciplinary Analysis and Optimization Conference*. American Institute of Aeronautics and Astronautics, 09 2006.
- [9] Burgio G., Mangeruca L., Ferrari A., Yapi L., “Framework for modelling and Simulation of multi-physics aircraft systems with distributed electronic controllers”. In: *Conference: AeroTech Congress & Exhibition*, September 2017.
- [10] Stephen C J. “Flight test experience with an electromechanical actuator on the F-18 systems research aircraft”. NASA.1998.
- [11] L. Jun, F. Yongling, P. Zhongcai, L. Wangyu, X. Buli. “Current Practice and New Development of Airborne Integrated Actuation System, Machine Tool & Hydraulic”, 2004, No.1.
- [12] Jackson D. “Robust Aircraft Subsystem Conceptual Architecting”, *Ph.D. thesis*; Georgia Institute of Technology; Atlanta 2013, GA, USA.

- [13] A. Fraj, M. Budinger, T. El Halabi, JC. Maré, GC. Negoita. “Modelling approaches for the simulation-based preliminary design and optimization of electromechanical and hydraulic actuation systems”. In: *53rd AIAA/ASME/ASCE/AHS/ASC Structures, Structural Dynamics and Materials Conference 20th AIAA/ASME/AHS Adaptive Structures Conference 14th AIAA*. Honolulu, Hawaii; 2012. p. 1523.
- [14] I. Chakraborty, D. Jackson, D. Trawick, D. Mavris. “Development of a Sizing and Analysis Tool for Electro-hydrostatic and Electromechanical Actuators for the More Electric Aircraft”. In: *2013 Aviation Technology, Integration, and Operations Conference*. Los Angeles, CA: AIAA Aciation; 2013. p. 4282.
- [15] J. Liscouët, JC. Maré, M. Budinger. “An integrated methodology for the preliminary design of highly reliable electromechanical actuators: Search for architecture solutions”. *Aerospace Science and Technology*. 2012; 22(1): 9–18.
- [16] CRESCENDO. “Collaborative and Robust Engineering using Simulation Capability Enabling Next Design Optimisation”. Final Report Summary, 2013. Website: <http://cordis.europa.eu/result/rcn/140562>. Last access: 2017-05-30.
- [17] TOICA. “Thermal Overall Integrated Conception of Aircraft”. Final Report Summary, 2017. Website: <http://cordis.europa.eu/project/rcn/110079>. Last access: 2017-05-31.
- [18] MOET. “More Open Electrical Technologies”. Project details, 2011. Website: <http://cordis.europa.eu/project/rcn/814721>. Last access: 2017-05-31.
- [20] Aeronautics Guide - Powered by Blogger. Website: http://okigihan.blogspot.com/p/aircraft-brakes_9081.html.
- [21] E. Nihad Daidzic. “Modeling and Computation of the Maximum Braking Energy Speed for Transport Category Airplanes”. In *Journal of Aviation Technology and Engineering* 6:2 (2017) 2-25.
- [22] MOOG. “ELECTRO-HYDRAULIC VALVES: A TECHNICAL LOOK”. Website: <http://www.moogvalves.com/uk/tech-look/webserv/infographic-16404N-4148ZT.html>.
- [23] Pier Carlo Berri. “Genetic Algorithms for Prognostics of Electromechanical Actuators”. In *Master degree thesis*. Politecnico di Torino, October 2016.
- [24] A. Garcia Garriga, P. Govindaraju, S.S. Ponnusamy, N. Cimmino, L. Mainini. “A modelling framework to support power architecture trade-off studies for More-Electric Aircraft”. *Transportation Research Procedia*, vol. 29, 2018, pp. 146-156.
- [25] Brian E. St. Rock, Larry E. Zeidner, Niranjana A. Desai and Hayden M. Reeve. United Technologies Research Center, East Hartford, CT 06108, USA Michael P. Strauss. Sikorsky Aircraft, Stratford, CT 06615, USA.

- [26] A. Garcia Garriga, S.S. Ponnusamy, L. Mainini. “A multi-fidelity framework to support the design of More-Electric Actuation”. In: *Proceedings of 2018 Multidisciplinary Analysis and Optimization Conference*, AIAA Aviation Forum, June 25-29, 2018, Atlanta GA.
- [27] MICHELIN AIRCRAFT TYRE. “Aircraft Tyre, Engineering Data”. # REFERENCE: MAT-DB-01, Rev A.
- [28] Federal Aviation Administration Regulation. “Pilot Guide to Takeoff Safety” Website: https://www.faa.gov/other_visit/aviation_industry/airline_operators/training/media/takeoff_safety.pdf.
- [29] Shuai Wu, Bo Yu, Zongxia Jiao, Yaoxing Shang. “Preliminary design and multi-objective optimization of electro-hydrostatic actuator”. In *Institution of Mechanical Engineers, Part G: Journal of Aerospace Engineering*. 2016, Vol 231, Issue 7, pp. 1258 - 1268.
- [30] Miller Fluid Power. “Application Engineering Guide”. File 9905 070108.
- [31] EATON Power Business Worldwide. “Eaton’s Pump and Motor Products: Catalog”. Document No. M-HYOV-MC003-E1.
- [32] ACTUATION2015 website. Website: <http://www.actuation2015.eu/>.
- [33] Marc Budinger. “Preliminary design and sizing of actuation systems”. Mechanical engineering [physics.class-ph]. UPS Toulouse, 2014.
- [34] Nihad E. Daidzic and Juna Shrestha. “Airplane Landing Performance on Contaminated Runways in Adverse Conditions”. State University, Mankato, Minnesota 56001.
- [35] ESI ITI GmbH. “Library Manual - SimulationX”. Website: <https://www.esi-group.com/>.
- [36] ESI ITI GmbH. “SimulationX: Training Modeling and Simulation of Hydraulic Systems”. Website: <https://www.esi-group.com/>.
- [37] Georgia Institute of Technology, OpenHydraulics - licensed by GitHub. Website: <https://github.com/cparedis/OpenHydraulics>.
- [38] A. Wohnhaas, D. Hötzer, U. Sailer. “Modulares Simulationsmodell eines Kfz-Antriebsstranges unter Berücksichtigung von Nichtlinearitäten und Kupplungsvorgängen”. In *VDI Berichte* Nr. 1220, Schwingungen in Antrieben, VDI-Verlag GmbH, Düsseldorf, 1995.
- [39] M. Otter, N. Thuy, D. Bouskela, L. Buffoni, H. Elmqvist, P. Fritzson, A. Garro, A. Jardin, H. Olsson, M. Payelleville, W. Schamai, E. Thomas, A. Tundis. “Formal Requirements Modeling for Simulation-Based Verification”. In: *11th International Modelica Conference* September 21-23, 2015, Versailles, France.
- [40] Federal Aviation Administration Regulation. “FLIGHT TEST GUIDE FOR CERTIFICATION OF TRANSPORT CATEGORY AIRPLANES”. Website: https://www.faa.gov/documentLibrary/media/Advisory_Circular/25-7B.pdf.

- [41] GOOD YEAR AVIATION. “The Aircraft Tire DataBook”. Website:
<https://www.goodyearaviation.com/resources/tiredatabook.html>.
- [42] Van Den Bossche D. “The A380 flight control electro-hydrostatic actuators, achievements and lessons learnt”. In: *Proc. 25th Congress of the International Council of the Aeronautical Sciences*. 2006.
- [43] Dynardo GmbH, Weimar. “Methods for multi-disciplinary optimization and robustness analysis”. February 11, 2018.
- [44] Saltelli A. et al. “Global Sensitivity Analysis. The Primer”. Chichester, England: John Wiley & Sons, Ltd. 2008.
- [45] Dynardo - dynamic software & engineering, optiSLang - RTO software. Website:
<https://www.dynardo.de/en/software/optislang.html>.
- [46] Parker Hannifin Corporation. “Compact EHA Electro-Hydraulic Actuators for high power density applications”. Catalog HY22-3101E 7/13.
- [47] ROEMHELD, HILMA STARK, “Things Worth Knowing about Hydraulic Cylinders”. Website:
https://www.roemheldgruppe.de/fileadmin/user_upload/downloads/technische_informationen/Wissenswertes_Hydraulikzylinder_en_0212.pdf.
- [48] Parker-Hannifin Corporation, “NK Series, Frameless Servo Motor”. Website:
https://www.micromech.co.uk/uploads/assets/pdf/servo_motors/parker_servo_motor_nk_series.pdf.
- [49] M. McKay, R. Beckman, W. Conover. “A comparison of three methods for selecting values of input variables in the analysis of output from a computer code”. *Technometrics* 21, 239-245. 1979.
- [50] R. Iman and W. Conover. “A distribution-free approach to inducing rank correlation among input variables”. *Communications in Statistics - Simulation and Computation* 11,311-334. 1982.
- [51] Myers R. and Montgomery D. “Response Surface Methodology” (2 ed.). John Wiley & Sons, Inc. 2002.
- [52] L. Etman, J. Adriaens, M. Slagmaat, A. Schoofs. “Crashworthiness design optimization using multipoint sequential linear programming”. *Structural Optimization* 12, 222-228. 1996.
- [53] Montgomery D. and Runger G. “Applied Statistics and Probability for Engineers” (Third ed.). John Wiley & Sons. 2003.

- [54] N. Cimmino, S.S. Pannusamy, A. Garcia Garriga, L. Mainini. "A Modelling and Simulation Framework for the Integrated Design of Aircraft Systems. Submitted to Proc. IMechE Part G Journal of Aerospace Engineering EUCASS 2017 Special Issue.
- [55] D. Briere, C. Favre, P. Traverse. "Electrical Flight Controls, From Airbus A320/330/340 to Future Military Transport Aircraft: A Family of Fault-Tolerant Systems"; Editor C.R. Spitzer; The Avionics Handbook; Second edition; 12; CRC Press LLC; Boca Raton, FL, 2001, USA.
- [56] C. Bauer, K. Lagadec, C. Bès, M. Mongeau. "Flight Control System Architecture Optimization for Fly-By-Wire Airliners"; Journal of Guidance, Control, and Dynamics; 30(4); pp. 1023-1029. 2007.

ACKNOWLEDGEMENTS

Desidero ringraziare la mia co-relatrice Laura Mainini per la sua guida, consulenza e enorme sostegno durante la stesura di questa tesi.

Un grazie speciale anche al mio supervisor tecnico Sangeeth Sagar Pannusamy per il supporto inestimabile, l'estrema pazienza e la disponibilità che mi ha concesso durante tutto il mio tirocinio. Vorrei esprimere il mio apprezzamento per tutto ciò che ho appreso e per le grandi esperienze che ho condiviso con i miei colleghi ed ora amici presso il centro di ricerca United Technologies Research Centre-Ireland.

Un sentito ringraziamento a mio padre e a mia madre, che con grossi sacrifici e forte incoraggiamento, mi hanno fatto arrivare alla fine di questo lungo percorso.

Infine, un grazie a tutti i miei amici e soprattutto al mio fedele compagno di fatiche e bevute Simone Gaia per avermi accompagnato in questi anni speciali.